Heavy Metals Induce Iron Deficiency Responses at Different Hierarchic and Regulatory Levels[1][OPEN]

Alexandra Lešková,[a,b,c] Ricardo F. H. Giehl,[a] Anja Hartmann,[a] Agáta Fargašová,[b] and Nicolaus von Wirén[a,2]

[a]Department of Physiology and Cell Biology, Leibniz Institute for Plant Genetics and Crop Plant Research, 06466 Gatersleben, Germany

[b]Department of Environmental Ecology, Faculty of Natural Sciences, Comenius University in Bratislava, 84215 Bratislava, Slovakia

[c]Department of Plant Physiology, Plant Science and Biodiversity Center, Slovak Academy of Sciences, 84523 Bratislava, Slovakia

ORCID IDs: 0000-0003-4587-2550 (A.L.); 0000-0003-1006-3163 (R.F.H.G.); 0000-0002-9660-4313 (A.H.); 0000-0001-6443-1887 (A.F.); 0000-0002-4966-425X (N.v.W.).

In plants, the excess of several heavy metals mimics iron (Fe) deficiency-induced chlorosis, indicating a disturbance in Fe homeostasis. To examine the level at which heavy metals interfere with Fe deficiency responses, we carried out an in-depth characterization of Fe-related physiological, regulatory, and morphological responses in Arabidopsis (*Arabidopsis thaliana*) exposed to heavy metals. Enhanced zinc (Zn) uptake closely mimicked Fe deficiency by leading to low chlorophyll but high ferric-chelate reductase activity and coumarin release. These responses were not caused by Zn-inhibited Fe uptake via IRON-REGULATED TRANSPORTER (IRT1). Instead, Zn simulated the transcriptional response of typical Fe-regulated genes, indicating that Zn affects Fe homeostasis at the level of Fe sensing. Excess supplies of cobalt and nickel altered root traits in a different way from Fe deficiency, inducing only transient Fe deficiency responses, which were characterized by a lack of induction of the ethylene pathway. Cadmium showed a rather inconsistent influence on Fe deficiency responses at multiple levels. By contrast, manganese evoked weak Fe deficiency responses in wild-type plants but strongly exacerbated chlorosis in *irt1* plants, indicating that manganese antagonized Fe mainly at the level of transport. These results show that the investigated heavy metals modulate Fe deficiency responses at different hierarchic and regulatory levels and that the interaction of metals with physiological and morphological Fe deficiency responses is uncoupled. Thus, this study not only emphasizes the importance of assessing heavy metal toxicities at multiple levels but also provides a new perspective on how Fe deficiency contributes to the toxic action of individual heavy metals.

The contamination of arable soils with heavy metals has become a worldwide concern due to the ever-increasing industrial demand for metals. In particular, mining, smelting, waste disposal, and also agriculture contribute to the emission and distribution of heavy metals in the environment, where they can exert a detrimental effect on plant growth (Nagajyoti et al., 2010). A large part of their adverse effects has been explained by the inhibition of enzyme activities, the production of reactive oxygen species, and the competition with other nutrients in various physiological processes (Shahid et al., 2014). Among the most affected nutrients is iron (Fe), which shares several similarities with other heavy metals regarding chemical structure, behavior, and availability in soils or uptake by plant roots. An excess of several heavy metals can induce chlorosis in younger leaves (Schaaf et al., 2006; Meda et al., 2007; Morrissey et al., 2009; Fukao et al., 2011; Wu et al., 2012), hence resembling the most typical visual symptom of Fe deficiency (Vert et al., 2002; Wu et al., 2012). Even in the absence of visual symptoms, heavy metals can negatively interfere with Fe homeostasis, as seen in the case of manganese (Mn; Allen et al., 2007; Lanquar et al., 2010). Induction of Fe deficiency by heavy metals is due, at least in part, to the broad substrate specificity of IRON-REGULATED TRANSPORTER 1 (IRT1), which can transport divalent metals, such as zinc (Zn), cobalt (Co), nickel (Ni), cadmium (Cd), and Mn, besides Fe (Connolly et al., 2002, 2003; Henriques et al., 2002; Vert et al., 2002; Nishida et al., 2011). As these heavy metals may outcompete Fe during root uptake, they promote Fe deficiency and increase the up-regulation of *IRT1*, which further favors an imbalanced uptake of

[1] This work was supported by Vedecká Grantová Agentúra (grant no. VEGA 1/0098/14 to A.F. and A.L.) and by the Deutsche Forschungsgemeinschaft (grant no. WI1728/21-1) to N.v.W.

[2] Address correspondence to vonwiren@ipk-gatersleben.de.

The author responsible for distribution of materials integral to the findings presented in this article in accordance with the policy described in the Instructions for Authors (www.plantphysiol.org) is: Nicolaus von Wirén (vonwiren@ipk-gatersleben.de).

A.L., R.F.H.G., A.F., and N.v.W. designed the experiments; A.L. performed all experiments with the assistance of R.F.H.G.; A.H. performed the principal component analysis; A.L., R.F.H.G., and N.v.W. analyzed the data and wrote the article with contributions of all the authors.

[OPEN] Articles can be viewed without a subscription.

www.plantphysiol.org/cgi/doi/10.1104/pp.16.01916

other metals over Fe. In fact, several studies have indicated that Fe deficiency is associated with deleterious effects caused by excess Cd or Zn and that the induction of Fe deficiency-responsive genes is required to counteract metal toxicity (Meda et al., 2007; Solti et al., 2008; Fukao et al., 2011; Pineau et al., 2012).

In order to overcome Fe limitation, plants have evolved different mechanisms to acquire Fe from sparingly available Fe precipitates (Giehl et al., 2009). Nongraminaceous plants employ a reduction-based mechanism, which involves the solubilization of ferric Fe via protons released into the rhizosphere followed by the subsequent reduction of Fe(III) by FERRIC REDUCTION OXIDASE2 (FRO2; Robinson et al., 1999; Connolly et al., 2003). As shown in Arabidopsis (*Arabidopsis thaliana*), ferrous Fe is then transported across the root plasma membrane of outer root cells by IRT1 (Vert et al., 2002). Recently, it was found that the Fe(II)- and 2-oxoglutarate-dependent dioxygenase FERULOYL-COA 6′-HYDROXYLASE (F6′H1) assists the reduction-based strategy by solubilizing ferric Fe from sparingly soluble sources (Rodríguez-Celma et al., 2013; Schmid et al., 2014; Schmidt et al., 2014). This enzyme is involved in the synthesis of coumarins, some of which, upon release to the rhizosphere, are able to mobilize Fe from insoluble precipitates (Fourcroy et al., 2014; Schmid et al., 2014). At the transcriptional level, Fe acquisition in nongraminaceous plants is coordinated by the cooperative action of the basic helix-loop-helix (bHLH) transcription factors FER-LIKE IRON DEFICIENCY INDUCED TRANSCRIPTION FACTOR (FIT) and bHLH38 and bHLH39 (Colangelo and Guerinot, 2004; Yuan et al., 2008; Wu et al., 2012). FIT also can interact with the transcription factors ETHYLENE-INSENSITIVE3 (EIN3) and ETHYLENE-INSENSITIVE3-LIKE1 (EIL1), which, similar to bHLH38 and bHLH39, enhance FIT-mediated Fe acquisition (Lingam et al., 2011). To avoid oxidative stress by uncontrolled Fe uptake, IRT1 DEGRADATION FACTOR1 (IDF1) mediates the degradation of the plasma membrane-bound IRT1 protein (Shin et al., 2013). Intracellular availability of Fe in roots is controlled by FERRITIN1 (FER1), which oxidizes and stores excess Fe in order to prevent Fe-dependent oxidative stress (Briat et al., 2010). Iron allocation, in turn, is regulated by bHLH100 and bHLH101 (Sivitz et al., 2012; Wang et al., 2013) and by the transcription factors POPEYE (PYE) and MYB DOMAIN PROTEIN10 (MYB10) and MYB72 (Long et al., 2010; Palmer et al., 2013). Although the Fe-sensing mechanism is not yet completely known, a class of Haemerythrin motif-containing Really Interesting New Gene and Zinc-finger proteins and BRUTUS (BTS) from rice (*Oryza sativa*) and Arabidopsis, respectively, have been proposed as iron sensors (Kobayashi et al., 2013; Selote et al., 2015). The E3 ligase BTS is involved in the Fe-dependent posttranslational regulation of PYE-like transcription factors (Selote et al., 2015). These transcription factors then interact with PYE, which, in turn, regulates the expression of genes involved in the intracellular and intercellular transport of Fe in the root stele, such as *FERRIC REDUCTION OXIDASE3* (*FRO3*), *NICOTIANAMINE SYNTHASE4* (*NAS4*), and *FERRIC REDUCTASE DEFECTIVE3* (*FRD3*; Durrett et al., 2007; Long et al., 2010; Palmer et al., 2013; Selote et al., 2015). The expression of *NAS4* is coregulated by MYB10 and MYB72 (Palmer et al., 2013). MYB72 also is involved in the regulation of the phenylpropanoid pathway, including the synthesis of coumarins (Zamioudis et al., 2014), thereby linking Fe acquisition and Fe allocation processes. Taken together, the aforementioned genes represent a set of Fe deficiency-responsive genes that act at different regulatory levels, some of which are sensitive to other heavy metals (van de Mortel et al., 2006; Wu et al., 2012).

Upon exposure to excess Zn, Cd, or Ni, Arabidopsis induces the two major Fe acquisition genes *IRT1* and *FRO2*, resembling a genuine Fe deficiency (Becher et al., 2004; van de Mortel et al., 2008; Fukao et al., 2011; Nishida et al., 2011; Shanmugam et al., 2011; Wu et al., 2012). Nevertheless, other studies using the same plant species found a strong repression of *IRT1* and *FRO2* in response to high Cd supply (Besson-Bard et al., 2009; Hermans et al., 2011). Moreover, investigations of Fe deficiency-related transcriptional markers upon metal excess have been expanded to transcription factors (van de Mortel et al., 2006, 2008; Hermans et al., 2011). Therein, the expression of the transcription factors *bHLH38/39/100/101*, *PYE*, and *MYB72* was found to be up-regulated under high Cd or Zn supply, suggesting that Cd- and Zn-induced Fe deficiency is initiated at a higher regulatory level. In contrast, Besson-Bard et al. (2009) found no evidence for the induction of major transcriptional regulators under elevated supplies of Cd. Such discrepancies among experiments with different or even the same metal emphasize the necessity to investigate a series of time points and heavy metal concentrations and to standardize the plant cultivation platform with a direct comparison with Fe-deficient plants. The comparability of conditions is unequivocal in order to assess how specifically particular Fe-regulated gene sets respond to different heavy metals.

The large plasticity observed in root system architecture (RSA) under different nutrient deficiencies, including Fe deficiency (Gruber et al., 2013; Giehl et al., 2014), suggests that architectural root traits also may exhibit a large variation after exposure to different heavy metals. In the case of copper, lateral root emergence turned out to be more sensitive to excess copper supplies than primary root elongation (Lequeux et al., 2010). In the case of Zn, changes in root traits depended more strongly on the applied Zn dose. Lower concentrations of Zn induced lateral root elongation and caused no further changes in RSA (Jain et al., 2013), while higher concentrations inhibited both primary and lateral root growth (Fukao et al., 2011; Richard et al., 2011). However, so far, root architectural responses have always been analyzed separately under Fe deficiency or metal excess (Lequeux et al., 2010; Giehl et al., 2012; Gruber et al., 2013; Jain et al., 2013; Yuan et al., 2013). Thus, it remains unclear to what extent changes in root morphology upon heavy metal exposure

resemble those occurring under Fe deficiency and whether such root morphological changes can be attributed to the induction of Fe deficiency.

In order to assess whether and the level at which heavy metals interfere with Fe deficiency responses, we designed an integrative approach for the in-depth characterization of Fe-related physiological, regulatory, and morphological responses in Arabidopsis exposed to heavy metals. Plants were cultivated under unified experimental conditions that caused visual Fe deficiency symptoms due to either a lack of Fe supply or an excess of Zn, Co, Ni, Cd, or Mn. We then analyzed Fe deficiency-related root and shoot physiological responses, RSA traits, and the transcriptional response of Fe-regulated genes, which allowed ranking metals according to their ability to induce Fe deficiency. This systematic analysis showed that the occurrence and the intensity of Fe deficiency responses evoked by the tested metals differ substantially and are manifested at multiple levels. Excess Zn mimics typical Fe deficiency responses almost at all levels, whereas Co, Ni, and Cd tweak distinct Fe-related processes and Mn undergoes the least specific interaction with Fe. This study represents not only a novel type of multilevel comparative assessment of heavy metal toxicity effects but also provides a new perspective on the extent to which Fe deficiency contributes to the toxic action of these heavy metals.

RESULTS

Induction of Fe Deficiency Symptoms in Shoots by Heavy Metals

The main goal of this study was to investigate the extent to which heavy metal-induced Fe deficiency responses contribute to metal toxicity in Arabidopsis. Therefore, we grew plants in the absence or presence of 75 μM Fe-EDTA and a range of Zn, Co, Ni, Cd, or Mn supplies to identify those metal concentrations that induced leaf chlorosis and/or shoot biomass decrease similar to that in Fe-deficient plants (Fig. 1). Plants cultivated under elevated supplies of Zn, Co, Ni, or Cd developed chlorosis in young leaves, which resembled the typical visual symptoms observed in Fe-deficient plants (Fig. 1A). As expected, the appearance of leaf chlorosis was accompanied by a significant decrease in chlorophyll levels, which, depending on the heavy metal supply, were comparable to those of plants grown on 0 μM Fe (Fig. 1B). Both low Fe supply and the excess supply of all tested heavy metals, particularly at their highest concentrations, decreased shoot biomass significantly (Fig. 1C). Despite the suppression of shoot biomass, high Mn supplies induced neither any visible sign of leaf chlorosis nor a significant decrease in chlorophyll concentrations (Fig. 1). In fact, even when plants were supplied with up to 2,000 μM Mn, no apparent leaf chlorosis was induced in plants (Supplemental Fig. S1). Instead, brown spots appeared on the leaves, which are indicative of Mn toxicity (Fecht-Christoffers et al., 2006; Williams and Pittman, 2010).

To assess whether the high supplies of heavy metals caused significant changes in elemental concentrations, a detailed elemental analysis of the shoots was carried out. By raising the supply of individual heavy metals in the growth medium, the levels of these elements increased considerably in plant shoots (Table I). Even though the highest supplies of Zn, Co, Ni, and Cd provoked visible leaf chlorosis and loss of chlorophyll to a similar extent as under no Fe supply, these heavy metals suppressed shoot Fe levels much less than the lack of Fe supply (Table I). In fact, in those cases in which a particular heavy metal induced visible symptoms of Fe deficiency and a similar drop in chlorophyll concentrations to that under Fe deficiency, Fe concentrations in the shoots did not fall below critical deficiency levels (Fig. 1; Table I; Giehl et al., 2012; Marschner, 2012; Gruber et al., 2013). Zn treatments slightly decreased Mn levels in addition to those of Fe, whereas Co reduced phosphorus (P), potassium (K), and Zn levels. Ni treatment decreased P, K, and Mg levels, and Cd treatment decreased those of Zn and Mn and, at 40 μM supply, additionally those of calcium (Ca; Table I). Excess Mn did not affect Fe levels in the shoots but slightly decreased the concentrations of P and even more of Ca and especially of Mg to severely deficient levels. Thus, excess Mn supply provoked deficiency of Mg rather than of Fe. With the exception of Mn- and Cd-induced decreases in Ca and Mg concentrations, none of the other alterations in mineral element concentrations could be associated with symptoms typical of Fe deficiency in young leaves.

Since shoot Fe concentrations in metal treatments did not fall below the critical threshold, we assessed whether the severe chlorosis phenotype observed in these treatments was related to hampered Fe remobilization from source to sink tissues. Therefore, we conducted another experiment in which we measured Fe and metal concentrations in both young and old leaves separately. In fact, Fe concentrations in young leaves of metal-treated plants remained significantly above those in Fe-deficient plants (Supplemental Fig. S2A). With approximately 70 $\mu g\ g^{-1}$ Fe in young leaves of Zn-treated plants, young leaves also contained sufficient Fe for chlorosis-free growth. Furthermore, the ratio of Fe in old versus young leaves did not change relative to that in control or Fe-deficient plants (Supplemental Fig. S2B), indicating that Zn had no particular impact on Fe remobilization from old to young leaves. A different trend appeared in Co- or Cd-treated plants, in which these metals may have impaired Fe remobilization.

The next step was to verify whether metals alter Fe concentrations in the roots. We measured Fe and other heavy metal concentrations in roots after the removal of apoplastic Fe (Cailliatte et al., 2010; Zhai et al., 2014). While the concentrations of remaining Fe in roots may indicate that apoplastic Fe was not removed completely, all metal treatments significantly decreased Fe levels in the roots (Supplemental Fig. S3). Nevertheless,

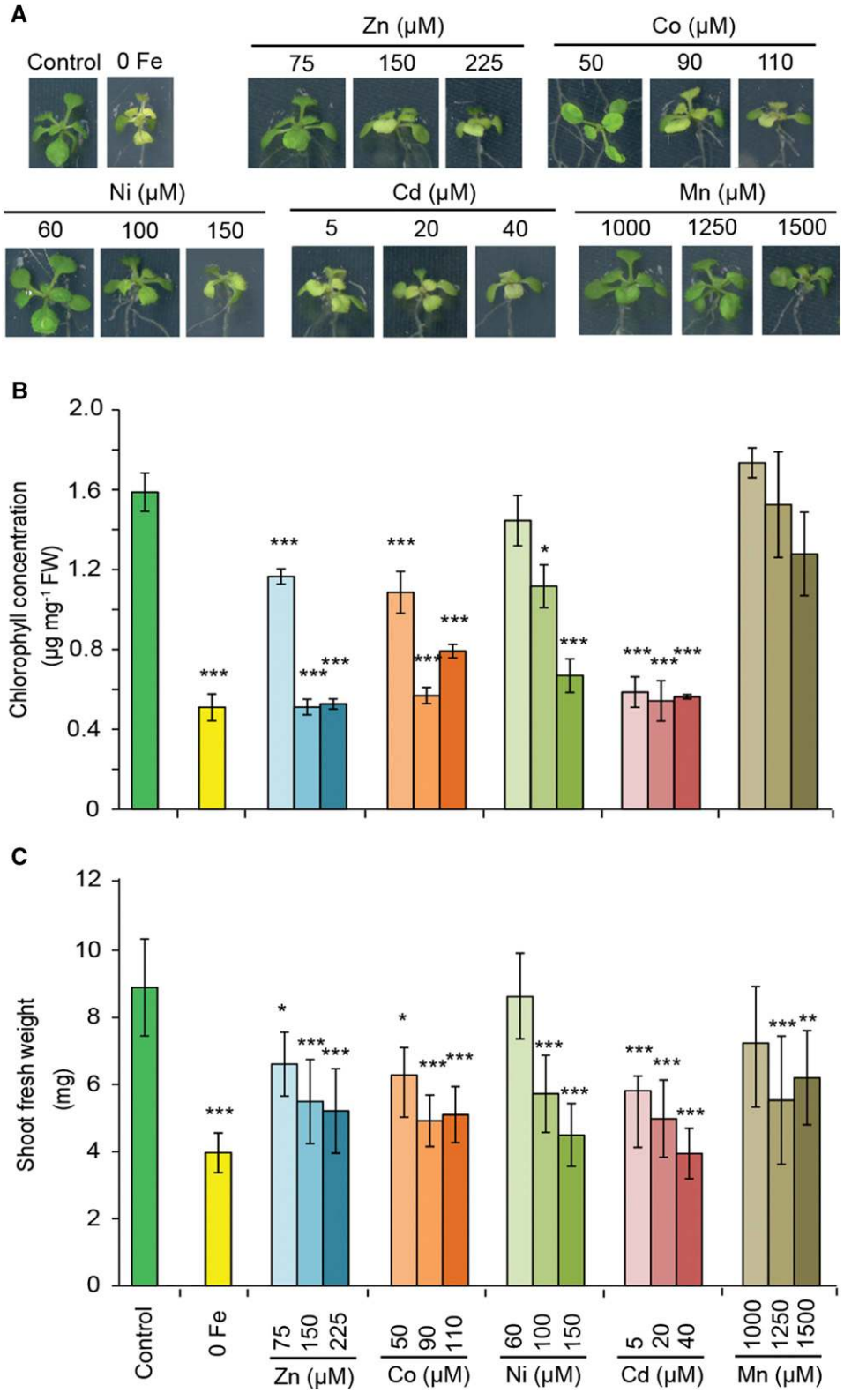

Figure 1. Appearance of typical Fe deficiency-related symptoms in Arabidopsis Columbia-0 (Col-0) plants exposed to various heavy metals. A, Shoot phenotypes. B, Chlorophyll concentrations of the shoots. C, Shoot fresh weights. Seedlings were precultured for 7 d in one-half-strength Murashige and Skoog (MS) medium and then transferred to one-half-strength MS medium with (control) or without Fe + 50 μM ferrozine (0 Fe) or with Fe and the supplementation of the indicated concentrations of different heavy metals. Plants were cultivated on these treatments for 9 d. Bars represent means ± SD; $n = 3$ to 4. Asterisks indicate statistically significant differences from the control treatment according to Tukey's test (*, $P < 0.05$; **, $P < 0.01$; and ***, $P < 0.001$). FW, Fresh weight.

remaining Fe levels in metal-treated plants were still 2-fold higher than under no Fe supply, rendering it unlikely that metal treatments led directly to deficient Fe levels in roots.

In order to verify whether the added heavy metals may have altered Fe availability by displacing Fe from highly soluble Fe(III)-EDTA chelates, we first performed a theoretical metal speciation analysis by

Table I. *Elemental concentrations in shoots of Arabidopsis plants grown on various concentrations of heavy metals*

Seedlings were precultured in one-half-strength MS medium for 7 d and then transferred to one-half-strength MS medium (control) or one-half-strength MS medium supplemented with the indicated concentrations of metals for 9 d. Values represent means ± SD. Different letters indicate statistically significant differences among means for each heavy metal ($P < 0.05$, Tukey's test); n.d., not detected. Boldface values are significantly lower than those measured in Fe-supplemented control plants. Values for Ca, K, Mg, P, and S are in mg g^{-1}, and those for Fe, Cd, Co, Mn, Ni, and Zn in μg g^{-1}.

Treatment		Ca	K	Mg	P	S	Fe	Cd	Co	Mn	Ni	Zn
	μM											
Fe	75	5.8 ± 0.4 b	53.5 ± 3.2 b	1.8 ± 0.1 b	15.7 ± 1.3 a	8.2 ± 0.4 a	89.7 ± 6.6 a	n.d.	n.d.	213 ± 14.4 b	n.d.	162 ± 15.0 b
	0[a]	9.9 ± 1.6 a	60.7 ± 8.3 a	2.7 ± 0.5 a	15.9 ± 2.2 a	21.3 ± 3.6 b	**19.3 ± 10.7 b**	n.d.	n.d.	456 ± 52.3 a	n.d.	1,006 ± 234.3 a
Zn	18	5.1 ± 0.7 b	54.1 ± 3.8 b	1.4 ± 0.1 ab	14.3 ± 1.1 a	8.6 ± 0.6 b	89.7 ± 6.6 a	n.d.	n.d.	199 ± 11.2 b	n.d.	157 ± 9.3 d
	75	6.1 ± 0.4 a	63.1 ± 4.4 a	1.5 ± 0.1 a	14.8 ± 1.9 a	13.5 ± 1.7 ab	**65.9 ± 11.3 b**	n.d.	n.d.	220 ± 16.8 a	n.d.	641 ± 160.7 c
	150	6.0 ± 0.8 a	56.2 ± 5.1 b	1.5 ± 0.1 ab	13.8 ± 1.3 a	17.1 ± 1.4 a	**54.3 ± 22.3 b**	n.d.	n.d.	184 ± 20.0 b	n.d.	1,060 ± 90.7 b
	225	5.1 ± 0.4 b	52.7 ± 5.4 b	1.3 ± 0.1 b	12.8 ± 1.7 a	16.6 ± 1.3 a	**63.4 ± 17.7 b**	n.d.	n.d.	**158 ± 14.9 c**	n.d.	1,325 ± 81.9 a
Co	0.05	4.0 ± 6.3 b	51.9 ± 4.2 a	1.6 ± 0.1 b	13.3 ± 1.3 a	10.0 ± 0.6 c	89.7 ± 6.6 a	n.d.	n.d. d	191 ± 14.9 a	n.d.	161 ± 33.7 a
	50	4.9 ± 5.5 a	49.3 ± 3.5 ab	1.8 ± 0.1 a	12.9 ± 1.3 ab	15.2 ± 0.7 a	82.2 ± 5.4 a	n.d.	197 ± 18.9 c	210 ± 17.0 a	n.d.	**116 ± 26.8 b**
	90	4.6 ± 2.0 a,b	**45.9 ± 2.2 b**	1.6 ± 01. a,b	**11.5 ± 1.2 b,c**	14.6 ± 0.9 a,b	**56.8 ± 14.8 b**	n.d.	328 ± 23.8 b	208 ± 10.1 a	n.d.	**111 ± 2.1 b**
	110	3.9 ± 4.9 b	**45.4 ± 1.4 b**	1.5 ± 0.1 b	**10.9 ± 1.0 c**	13.7 ± 0.6 b	**58.0 ± 9.7 b**	n.d.	406.9 ± 30.9 a	201 ± 12.3 a	n.d.	113 ± 5.6 a,b
Ni	0	2.7 ± 0.3 b	49.9 ± 3.8 b	1.3 ± 0.1 a	12.0 ± 1.2 a	8.0 ± 0.5 b	89.7 ± 6.6 a	n.d.	n.d.	166 ± 15.3 b	n.d. d	169 ± 24.2 c
	60	3.4 ± 0.5 a	58.3 ± 7.8 a,b	1.1 ± 0.1 a,b,c	13.5 ± 1.6 a	11.2 ± 1.8 a	75.6 ± 8.6 ab	n.d.	n.d.	225 ± 34.0 a	80 ± 13.7 c	330 ± 50.4 a
	100	2.4 ± 0.3 b	55.0 ± 2.5 a	**1.1 ± 0.1 b**	**9.4 ± 0.9 b**	9.7 ± 0.7 a	**71.2 ± 6.8 b,c**	n.d.	n.d.	146 ± 12.1 b	140 ± 16.9 b	245 ± 16.9 b
	150	3.1 ± 0.4 a	**39.6 ± 3.3 c**	**1.0 ± 0.1 c**	**7.4 ± 0.8 b**	8.7 ± 1.4 a	**49.9 ± 12.2 c**	n.d.	n.d.	118 ± 11.8 b	296 ± 36.2 a	192 ± 37.4 b
Cd	0	5.0 ± 0.3 b	50.0 ± 1.8 b	1.6 ± 0.1 c	14.2 ± 0.9 c	8.4 ± 0.5 c	89.7 ± 6.6 a	n.d. c	n.d.	211 ± 15.0 b	n.d.	169 ± 23.2 a
	5	7.8 ± 0.6 a	68.8 ± 4.9 a	2.2 ± 0.1 a	20.4 ± 2.0 a	18.3 ± 2.2 b	**61.0 ± 8.9 b**	200 ± 35.7 b	n.d.	235 ± 13.8 a	n.d.	165 ± 16.4 a
	20	4.3 ± 0.4 b	58.4 ± 5.0 ab	1.8 ± 0.2 b	16.8 ± 1.1 b	24.2 ± 2.4 a	**65.2 ± 12.5 b**	238 ± 30.0 a,b	n.d.	**139 ± 13.7 c**	n.d.	149 ± 38.4 ab
	40	**3.3 ± 0.3 c**	52.3 ± 2.4 b	1.6 ± 0.1 b,c	16.2 ± 1.1 b	21.3 ± 1.5 a,b	**66.3 ± 18.4b**	280 ± 15.7 a	n.d.	**118 ± 13.5 c**	n.d.	**118 ± 10.5 b**
Mn	40	3.2 ± 0.1 b	46.1 ± 2.2 a	1.2 ± 0.05 a	8.7 ± 0.3 a	6.4 ± 0.3 c	89.7 ± 6.6 a	n.d.	n.d.	143 ± 8.7 c	n.d.	128 ± 23.4 b
	1,000	2.1 ± 0.3 b	48.4 ± 6.0 a	**0.6 ± 0.05 b**	8.8 ± 1.3 a	10.1 ± 0.9 a	83.8 ± 12.7 a	n.d.	n.d.	2,261 ± 286.4 b	n.d.	228 ± 18.4 a
	1,250	2.7 ± 0.8 b	51.7 ± 6.7 a	**0.6 ± 0.2 b,c**	**6.1 ± 0.6 b**	7.8 ± 0.4 b	74.7 ± 15.7 a	n.d.	n.d.	2,785 ± 386.0 a,b	n.d.	207 ± 19.1 a
	1,500	**1.3 ± 0.4 c**	47.4 ± 2.5 a	**0.5 ± 0.1 c**	**7.5 ± 0.7 b**	10.3 ± 0.5 a	75.4 ± 13.1 a	n.d.	n.d.	2,650 ± 135.5 a	n.d.	235 ± 20.3 a
Critical values[b]		5 - 3	50 - 20	3.5 - 1.5	5 - 3	5 - 1	150 - 50	–	–	20 - 10	10 - 0.01	20 - 15

[a]0 Fe + 50 μM ferrozine. [b]According to Marschner (2012) and Gruber et al. (2013).

simulating the elemental composition of the different agar media used in our experiments. According to a simulation carried out with Visual MINTEQ 3.1 software (Gustaffson, 2012), the presence of metals provoked no or only little displacement of Fe from Fe(III)-EDTA complexes (3% or less) except for Ni, which lowered Fe availability by 10% (Supplemental Table S1). Therefore, we directly compared plant responses to heavy metals when Fe was supplied as Fe(III)-EDTA or Fe(III)-EDDHA. Fe(III)-EDDHA is more stable than Fe(III)-EDTA (pK of 35.1 versus 25.1, respectively; Smith and Martell, 1989) and more resistant to photodegradation (Yunta et al., 2003). According to Fe and chlorophyll concentrations, Zn and Ni induced leaf chlorosis to a highly similar extent when supplemented with Fe(III)-EDTA or Fe(III)-EDDHA (Supplemental Fig. S4). Therefore, a reduced Fe availability prior to uptake was unlikely to contribute to the heavy metal-induced Fe deficiency responses.

Effects of Excess Heavy Metals on Physiological Root Responses to Fe Deficiency

In the next step, we assessed whether heavy metal-induced stress is associated with typical Fe deficiency-related physiological responses in roots and focused on ferric chelate reduction. Plants were subjected to metal concentrations shown to induce Fe deficiency symptoms after 9 d (Fig. 1; Table I). Already after 3 d of metal exposure, the expression of *FRO2*, which is responsible for most of the Fe deficiency-induced ferric-chelate reductase (FCR) activity in Arabidopsis roots (Robinson et al., 1999), was induced by high Zn and Co almost to the same degree as by Fe deficiency (Fig. 2A). Transcript levels of this gene also were up-regulated by all other heavy metals, although to a lesser extent. During the time course of metal exposure, *FRO2* transcript levels dropped markedly, but they remained higher in roots of plants grown on low Fe or excess Zn (Fig. 2A). As expected, the high levels of *FRO2* expression in Fe-deficient roots were accompanied by higher FCR activities (Fig. 2B). In agreement with the induction of *FRO2* expression, also high Zn and Co provoked significant increases in FCR activities. In the case of Co, however, such an induction was limited to the first time point (Fig. 2B). Ni also induced FCR activity, although to a lower extent than low Fe or high Zn and Co. Roots treated with high Mn experienced only a slight increase in *FRO2* transcript levels and FCR activity (Fig. 2). The weak but significant up-regulation of *FRO2* expression by Cd excess was not translated into increased FCR activities at any time point.

Recently, it was shown that Fe deficiency induces the synthesis and release of coumarins in roots of Arabidopsis (Rodríguez-Celma et al., 2013; Fourcroy et al., 2014; Schmid et al., 2014). However, it is not yet known whether excess heavy metals also can induce such a response. Therefore, we first assessed the responsiveness of *F6′H1* to excess heavy metals (Fig. 3A). As

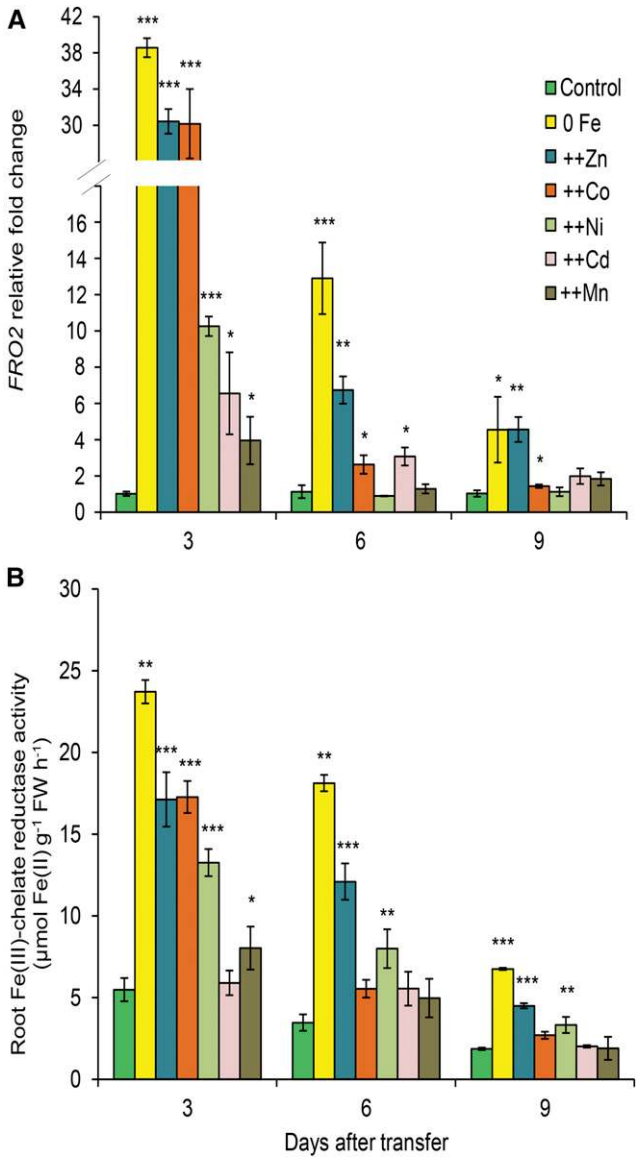

Figure 2. *FRO2* expression and root Fe(III)-chelate reductase activity in response to heavy metal supplies. Time-course analysis is shown for *FRO2* transcript levels (A) and root Fe(III)-chelate reductase activities (B) of plants exposed to different treatments. Seven-day-old seedlings grown on one-half-strength MS medium were transferred to one-half-strength MS medium with (control) or without Fe + 50 μM ferrozine (0 Fe) or with Fe and supplemented with 225 μM Zn (++Zn), 110 μM Co (++Co), 100 μM Ni (++Ni), 5 μM Cd (++Cd), or 1,500 μM Mn (++Mn). Bars represent means ± SE; n = 5 to 6. Asterisks indicate statistically significant differences from controls at each time point according to Tukey's test (*, $P < 0.05$; **, $P < 0.01$; and ***, $P < 0.001$). FW, Fresh weight.

expected, Fe deficiency up-regulated transcript levels of *F6′H1* during the whole course of the experiment. Zn and Co caused similarly high transcript levels of this gene at the earliest time point. However, *F6′H1* up-regulation by high Co was not sustained after prolonged exposure to this heavy metal. High Ni and high

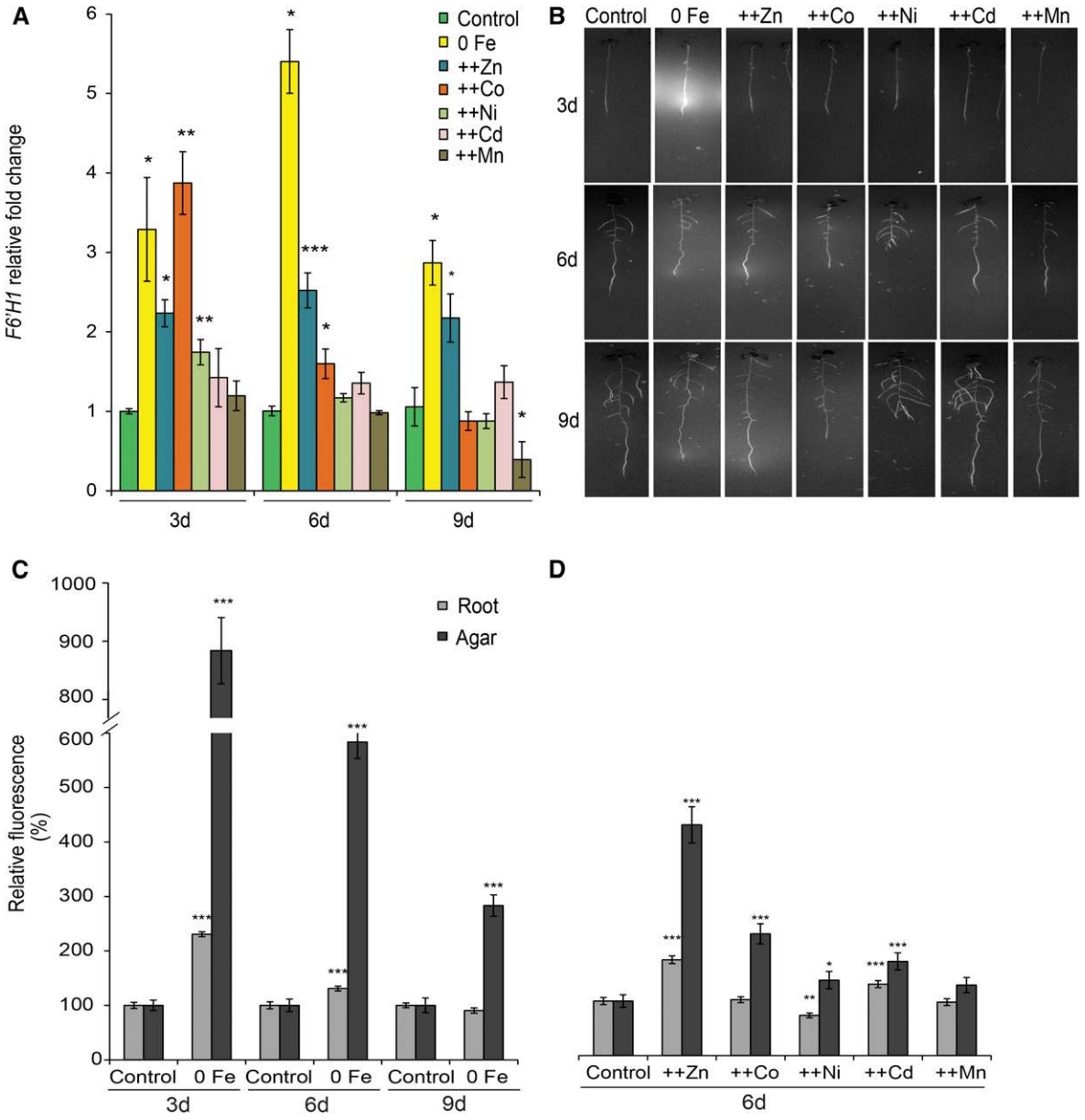

Figure 3. Effects of heavy metals on *F6′H1* gene expression and the accumulation of fluorescent coumarins in roots and root exudates. A, Time course of *F6′H1* transcript levels. B, UV fluorescence visualized at 365-nm wavelength. C and D, Relative fluorescence measured in roots and agar of plants grown on no supplementation of Fe + 50 μM ferrozine (0 Fe) for 3, 6, and 9 d (C) or excess heavy metal supplies for 6 d (D). Relative quantification was based on average pixel intensities of equally defined lengths of roots and agar portions around the roots. Seven-day-old seedlings grown on one-half-strength MS medium were transferred to one-half-strength MS medium with (control) or without Fe + 50 μM ferrozine (0 Fe) or with Fe and supplemented with 225 μM Zn (++Zn), 110 μM Co (++Co), 100 μM Ni (++Ni), 5 μM Cd (++Cd), or 1,500 μM Mn (++Mn). Bars represent means ± SE; $n = 25$ to 30. Asterisks indicate statistically significant differences from controls at each time point according to Tukey's test (*, $P < 0.05$; **, $P < 0.01$; and ***, $P < 0.001$).

Cd supplies caused only an initial slight up-regulation of *F6′H1*, whereas Mn caused either no induction or even a down-regulation, as evident over the long term (Fig. 3A). Many coumarins synthesized in response to low Fe availability exhibit fluorescence when exposed to UV light (365 nm), which allowed us to monitor the appearance of coumarin-dependent fluorescence in roots and in the agar (Fig. 3B). Compared with control conditions, the cultivation of plants without Fe supplementation resulted in a strong accumulation of fluorescence in roots and in the agar (Fig. 3, B and C). Although more pronounced at the first time point (i.e. 3 d after starting the treatments), the increased levels of fluorescence detected in the agar persisted over 9 d. None of the heavy metals provoked such a response at the earliest time point (Fig. 3B). However, excessive

supply of Zn provoked a significantly higher fluorescence in both roots and agar after a period of 6 d (Fig. 3, B and D). Co, Cd, and Ni supplies, in this order, caused less but still significant increases in agar fluorescence (Fig. 3, B and D). Thus, these heavy metals stimulated a moderate synthesis and secretion of fluorescent coumarins.

Altogether, these results indicated that Zn induced all root physiological responses typically associated with Fe deficiency, while Co and Ni moderately affected FCR activity and coumarin synthesis or release. In contrast, high Cd and Mn did not provoke prominent changes in Fe-related physiological root responses.

Effects of Excessive Heavy Metal Supplies on RSA

RSA is highly responsive to nutritional conditions and can be employed as a read-out for the plant nutritional status (Malamy, 2005; Giehl et al., 2014). Thus, we compared the RSA of plants grown under a range of Fe or heavy metal concentrations and assessed which RSA traits responded most sensitively to metals. Mild Fe deficiency, which was obtained by growing plants with the supply of 5 or 2.5 μM Fe-EDTA, caused a small but significant increase in primary root length and a slight increase in average lateral root length (Fig. 4A; Table II). Only when Fe concentrations in the growth medium dropped below 1 μM did the length of the lateral roots decrease significantly. Noteworthy, the addition of ferrozine, a potent Fe(II) chelator, to Fe-deficient medium resulted in an additional repression of primary root length. In contrast, lateral root density decreased consistently with decreasing Fe supplies, suggesting that this root trait is the most sensitive to Fe limitation (Fig. 4A; Table II).

Increasing supplies of all tested heavy metals reduced root growth and altered the plants' RSA, to some degree, in a metal-dependent manner (Fig. 4, B–F; Table II). With regard to lateral root density, the Co and Ni treatments were most clearly set apart from the Fe deficiency response, because lateral root densities increased with increasing Co or Ni supplies (Fig. 4, C and D; Table II). In the case of Ni, the most sensitive RSA component was primary root length, as a significant decrease in primary root length was recorded before any change in lateral root density or average lateral root length was detected (Fig. 4D; Table II). In general, decreasing primary root and lateral root lengths were observed with all metal treatments without any initial increase at lower metal doses, as observed under mild Fe deficiency. Increasing the supply of Zn and Cd led to prominent decreases in primary root length and lateral root density, which appeared to progress more intensively than under Fe deficiency (Fig. 4, B and E; Table II). Also, average lateral root length responded more sensitively to elevated doses of Zn and Cd than to a shortage in Fe supply. Unlike Zn and Cd, excess Mn induced more similar root architectural changes to those seen under progressing Fe deficiency, since the repression of lateral root density and average lateral root length set in before Mn caused any effect on primary root length (Fig. 4F; Table II).

In order to capture the major trends in the variation of RSA traits under the metal treatments tested in this study, we conducted a principal component analysis (PCA) of the measured root traits. According to PCA, principal component 1 (PC1) and principal component 2 (PC2) explained 58% and 35% of the variation of the measured traits among the treatments, respectively (Fig. 5A). In order to determine how much each principal component is loaded by individual root traits, we conducted Pearson's correlation analysis between root traits and principal components. PC1 was highly correlated with primary and lateral root lengths, while PC2 was strongly determined by variations in lateral root density (Fig. 5B). Most clearly, high Ni and Co treatments separated from Fe deficiency and other metal treatments along PC2. This was reflected by the prominent increase in lateral root density under high Ni and Co. In fact, on the PCA plot, the gradual decrease in root trait variability under decreasing Fe supply mostly overlapped with those observed at increasing levels of Mn (Fig. 5A). Only at higher doses of Mn (1,500 μM or greater) did root traits separate more along PC2. Initially, RSA trait changes under Zn and Cd excess also followed a similar pattern to that in Fe treatments; however, variations in RSA traits observed already at greater than 150 μM Zn or greater than 20 μM Cd were distributed farther along PC1 than those obtained under decreasing Fe supplies. This indicated that a growing excess of heavy metals led to more severe changes in root phenotypes than were achieved upon limiting Fe supplies. Considering the direction and distance by which PCA clusters moved under increasing metal supplies, this analysis indicated that the pattern of RSA trait changes, especially under Mn and, to a lesser extent, under Zn and Cd excess, mostly resembled those induced by Fe deficiency, whereas Co- and Ni-induced changes were most distinguishable.

Impact of Foliar Fe Supply and IRT1-Mediated Fe Uptake on Heavy Metal-Induced Physiological and Morphological Responses

To assess whether plant responses to heavy metals were indicative of a systemic Fe deficiency status, we supplied Col-0 plants grown under excess Zn, Ni, or Mn with foliar Fe. By alleviating chlorosis, preventing FCR activation, and inhibiting primary and lateral root elongation (Fig. 6, A–D), foliar Fe supply reversed almost all Fe deficiency-related responses provoked by high-Zn treatment, even though Zn still overaccumulated heavily in shoots (Supplemental Fig. S5). This may be indicative of a direct interaction of Zn with systemic Fe signaling. Only suppressed lateral root density evoked by high Zn supply was not reversed by foliar Fe treatment (Fig. 6E), which was related to the fact that the lateral root density of control plants even decreased by foliar Fe supply and showed an opposite response to other root

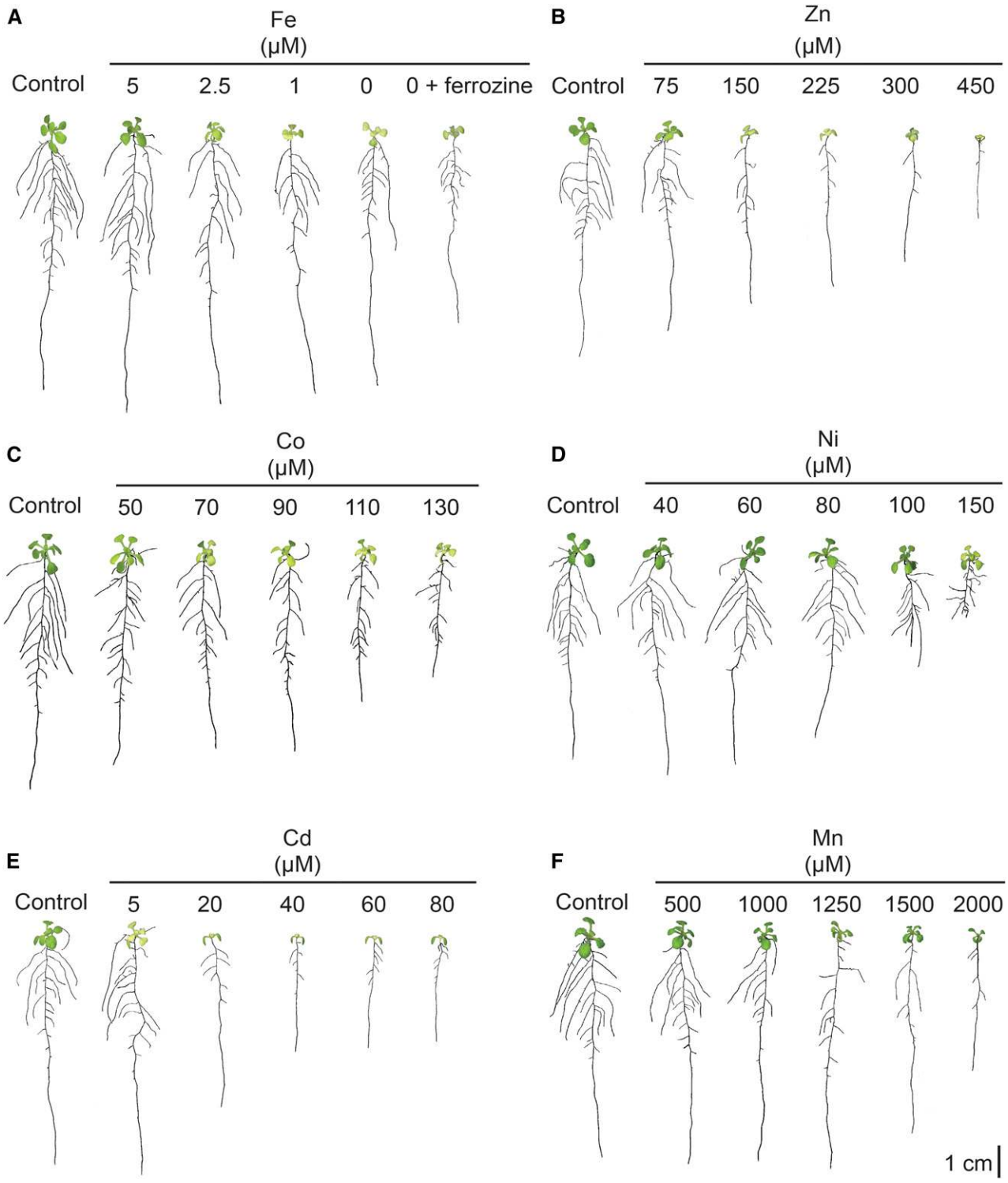

Figure 4. RSA of Arabidopsis in response to elevated heavy metal supplies and low Fe. Seedlings were exposed to different concentrations of Fe (A), Zn (B), Co (C), Ni (D), Cd (E), or Mn (F). Representative plants for each treatment are shown; $n = 30$ to 40. Seedlings were precultured for 7 d in one-half-strength MS medium and then transferred to one-half-strength MS medium (control) or one-half-strength MS medium containing the indicated concentration of each metal for a further 10 d.

traits. In contrast, foliar supply of Fe to high-Mn-treated plants did not affect any of the measured traits (Fig. 6). In addition, foliar Fe supply to Ni-treated plants had no impact on morphological root traits (Fig. 6, C–E), although Fe application fully recovered shoots from chlorosis and prevented the activation of FCR (Fig. 6,

Table II. *Primary root length, lateral root density, and average lateral root length of plants grown on various concentrations of heavy metals*

Values represent means ± SD. Different letters indicate statistically significant differences among means for each heavy metal ($P < 0.05$, Tukey's test).

Treatment			Primary Root Length	Lateral Root Density	Average Lateral Root Length
	μM		*cm root*$^{-1}$	*no. cm*$^{-1}$ *primary root*	*cm root*$^{-1}$
Fe	75	(control)	8.5 ± 0.8 b	2.9 ± 0.5 a	0.8 ± 0.2 a,b
	5		9.2 ± 0.9 a	2.4 ± 0.5 b	1.0 ± 0.2 a
	2.5		8.9 ± 0.8 a	2.3 ± 0.4 b,c	0.9 ± 0.2a
	1		8.6 ± 0.9 a,b	1.8 ± 0.5 d	0.7 ± 0.2 b,c
	0		8.0 ± 1.0 b,c	1.6 ± 0.3 d	0.7 ± 0.2 c
	0	+ ferrozine	6.5 ± 0.8 c	1.8 ± 0.5 c,d	0.6 ± 0.2 c
Zn	18	(control)	7.4 ± 0.6 a	2.7 ± 0.4 a	0.7 ± 0.2 a
	75		6.4 ± 0.6 b	2.7 ± 0.5 a	0.6 ± 0.1 b
	150		5.5 ± 0.7 c	2.0 ± 0.4 b	0.4 ± 0.1 c
	225		4.8 ± 0.5 d	1.6 ± 0.4 b	0.3 ± 0.1 d
	300		4.0 ± 0.7 e	1.5 ± 0.5 b	0.2 ± 0.1 d,e
	450		2.8 ± 0.4 f	1.7 ± 0.7 b	0.1 ± 0.1 e
Co	0.05	(control)	7.6 ± 0.4 a	2.9 ± 0.5 c	1.1 ± 0.2 a
	50		6.9 ± 0.8 b	3.0 ± 0.6 b,c	0.7 ± 0.2 b
	70		6.3 ± 1.0 b,c	3.5 ± 0.8 a,b	0.6 ± 0.2 b,c
	90		6.3 ± 1.0 c,d	3.5 ± 0.8 a	0.6 ± 0.2 c,d
	110		4.7 ± 1.1 d,e	3.7 ± 0.9 a	0.5 ± 0.2 d,e
	130		4.2 ± 1.1 e	4.1 ± 0.9 a	0.4 ± 0.1 e
Ni	0	(control)	7.0 ± 0.7 a	2.9 ± 0.5 b	0.9 ± 0.2 a
	40		7.3 ± 2.1 a	2.7 ± 1.5 b	0.9 ± 0.3 a
	60		6.9 ± 0.7 a	2.7 ± 0.4 b	0.8 ± 0.1 a
	80		6.1 ± 0.7 b	2.9 ± 0.5 b	0.8 ± 0.1 a
	100		2.8 ± 0.6 c	4.7 ± 1.4 a	0.8 ± 0.2 a
	150		2.2 ± 0.6 c	4.9 ± 1.6 a	0.3 ± 0.2 b
Cd	0	(control)	6.8 ± 1.1 a	2.7 ± 0.4 a	0.8 ± 0.2 a
	5		8.1 ± 1.0 a	2.3 ± 0.5 a	0.8 ± 0.2 a
	20		5.3 ± 0.5 b	1.2 ± 0.3 d	0.5 ± 0.2 b
	40		4.0 ± 0.5 b,c	1.6 ± 0.5 c	0.4 ± 0.1 c
	60		3.5 ± 0.3 c,d	1.9 ± 0.5 b,c	0.3 ± 0.1 c,d
	80		3.0 ± 0.3 d	2.3 ± 0.6 a,b	0.2 ± 0.1 d
Mn	40	(control)	7.5 ± 0.6 a	2.9 ± 0.3 a	0.8 ± 0.3 a
	500		7.9 ± 0.7 a	2.6 ± 0.3 a,b	0.8 ± 0.2 a,b
	100		7.4 ± 0.8 a	2.2 ± 0.4 b,c	0.6 ± 0.2 b,c
	1,250		8.1 ± 1.3 a	2.0 ± 0.6 c,d	0.5 ± 0.2 c
	1,500		6.3 ± 1.3 b	2.0 ± 0.5 c,d	0.5 ± 0.3 c
	2,000		4.4 ± 0.9 c	1.2 ± 0.6 d	0.2 ± 0.1 d

A, B, and F). Therefore, root architectural changes evoked by Ni (Fig. 4) clearly were not related to systemic Fe deficiency but rather caused by a local toxic effect of Ni.

Since IRT1 mediates the uptake of all heavy metals investigated here, we asked whether the differential effect of metals on Fe deficiency-related responses simply reflects an inhibition of IRT1-mediated Fe uptake by metals. Thus, we examined physiological and morphological responses to high Zn, Ni, and Mn in *irt1* mutant plants. Compared with wild-type plants, *irt1* mutants were not only affected by high Zn but more sensitive to high Ni and even to high Mn in terms of chlorophyll levels (Fig. 6, A and B). Notably, high Mn induced Fe deficiency at the physiological level specifically in *irt1* plants, as observed by a prominent increase in root FCR activity (Fig. 6F). The absence of functional IRT1 decreased the shoot levels of Fe and, to a lesser extent, those of Zn (Supplemental Fig. S5), indicating that, especially in the presence of excess metals, IRT1 contributed to Zn but not to Ni or Mn accumulation.

Finally, we tested whether those metal-induced physiological and morphological responses, which were independent of IRT1-mediated uptake, could be reversed by foliar Fe supply. In fact, Fe supply to *irt1* shoots brought back chlorophyll to wild-type levels and effectively repressed root FCR activity under excess Zn, Ni, or Mn (Fig. 6, A, B, and F), while shoot accumulation of these metals was not suppressed by leaf Fe supply (Supplemental Fig. S5). This substantial recovery suggested that the interference of metals with physiological responses was not caused at the level of IRT1 but rather regulated by metal-Fe interactions in the shoot. With regard to morphological root traits, foliar Fe did not prevent the occurrence of any of the metal-induced symptoms in *irt1* (Fig. 6, C–E), indicating that metal-induced root morphological changes in *irt1* were not affected by the plants' Fe nutritional status.

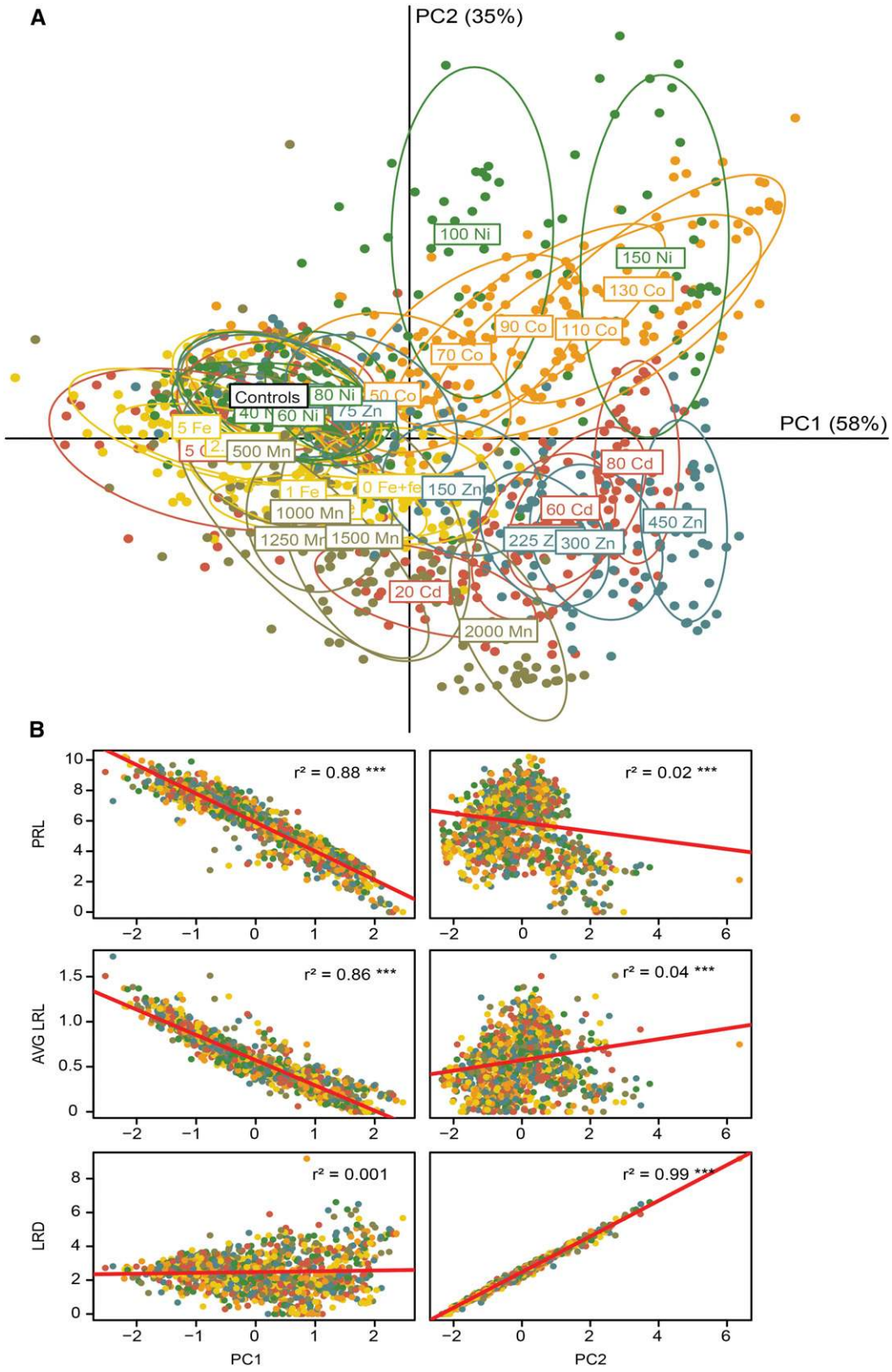

Figure 5. PCA of the variation in RSA traits in response to Fe deficiency and heavy metal supplies. PCA was based on primary root length (PRL), lateral root density (LRD), and average lateral root length (AVG LRL) measured under the indicated treatments. A, PC1, explaining 58% of the variation, was plotted against PC2, explaining 35% of the variation. B, Correlation analysis of root traits and principal components. r^2 values define coefficients of determination. Asterisks indicate statistical significance of the correlation between root traits and principal components: ***, $P < 0.001$.

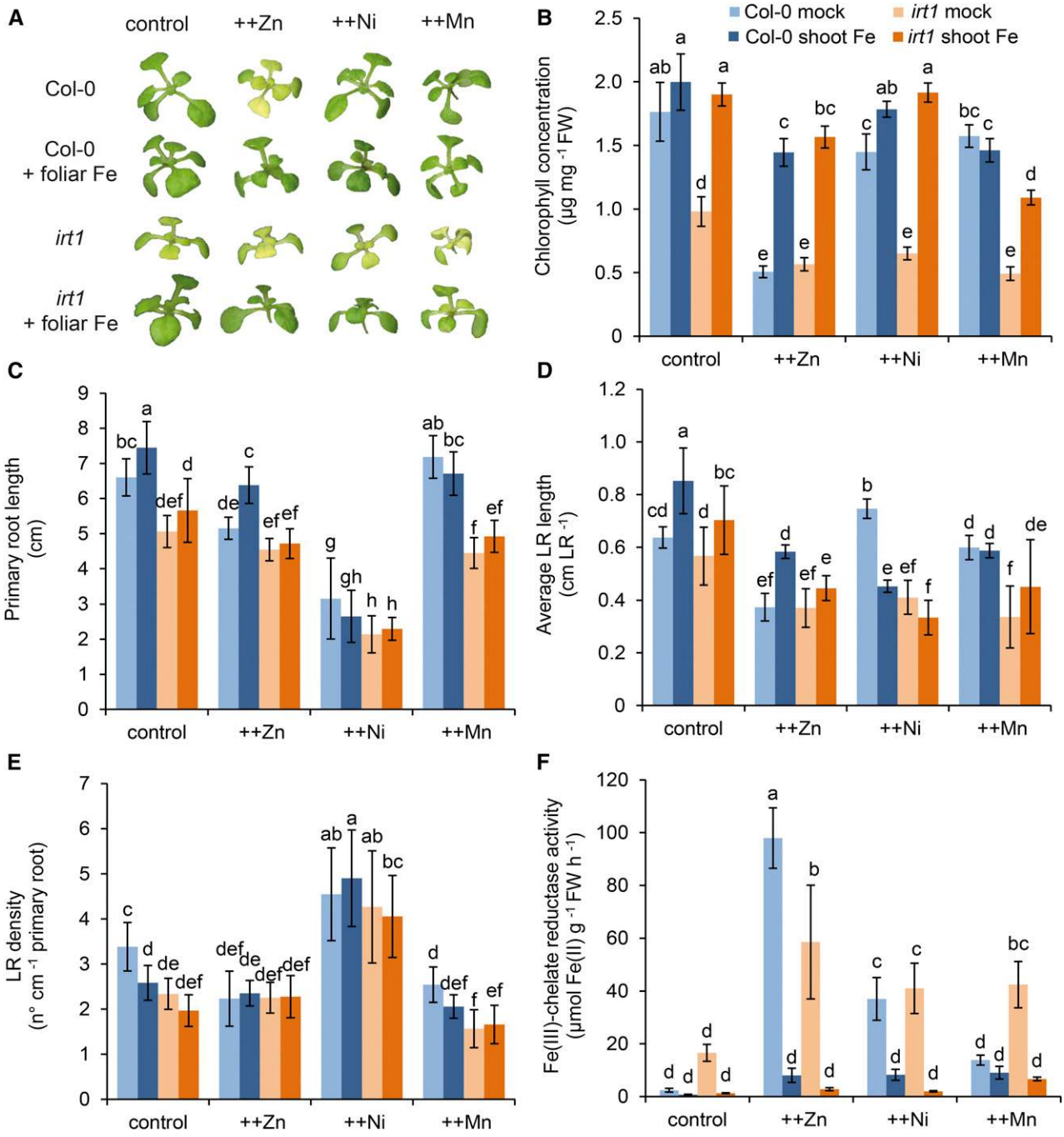

Figure 6. Effects of foliar Fe supply on the occurrence of heavy metal-induced physiological and morphological responses in Col-0 and *irt1*. Seven-day-old seedlings grown on one-half-strength MS medium were transferred to one-half-strength MS medium containing elevated concentrations of the indicated heavy metals. Leaves were supplied or not with 250 μM Fe(III) citrate. A, Appearance of plants. B, Chlorophyll concentration. C, Primary root length. D, Average lateral root (LR) length. E, Lateral root density. F, FCR activity. Bars represent means ± SD. Different letters indicate statistically significant differences among means for each heavy metal ($P < 0.05$, Tukey's test). FW, Fresh weight.

The Effect of Heavy Metals on the Expression of Fe Deficiency-Responsive Genes

In order to investigate whether individual heavy metals provoke Fe deficiency responses at the regulatory level, we assessed transcriptional changes in roots of 18 Fe deficiency-regulated genes in response to metal supplies (Fig. 7; Supplemental Table S2). Since it is difficult to establish comparable concentrations for the tested heavy metals, the expression analysis was carried out in a time course using two doses per heavy metal. By this procedure, we assessed how sensitively a

particular gene responded to increasing concentrations of and/or exposure time to a particular heavy metal. Relative to control conditions (one-half-strength MS medium supplied with 75 μM Fe), metal concentrations used in this experiment caused significant ($P < 0.05$) reductions in shoot fresh weight (Fig. 1C), chlorophyll concentrations (Fig. 1B), and shoot Fe concentrations (Table I). In the case of Mn, only the shoot fresh weight criterion was employed. For the normalization of transcript levels, we selected *UBIQUITIN2* (*UBQ2*) as a reference gene, since it showed the highest expression stability in response to the treatments used in this study (Supplemental Fig. S6).

In accordance with previous studies, 15 genes were either mildly or very strongly up-regulated as soon as 3 d after transferring plants to Fe-deficient conditions (Fig. 7). As expected, only transcript levels of *FER1*, which is induced by excess Fe and, hence, correlates positively with the Fe status of plants (Briat et al., 2010; Reyt et al., 2015), was consistently down-regulated in roots of Fe-deficient plants (Fig. 7). As the exposure time to Fe-deficient growth conditions progressed, the transcript levels of *IRT1* and *FRO2* and of the Fe-responsive bHLH-type transcription factors tended to decrease, whereas those of *EIL1*, *EIN3*, and *IDF1* rose more significantly at later time points.

Both tested Zn supplies produced transcriptional changes that resembled those triggered by Fe deficiency (Fig. 7). In particular, mRNA levels of all Fe deficiency-induced transcription factors experienced a strong up-regulation by high Zn even after prolonged exposure to this heavy metal. In the short term, high Co supply also was able to significantly induce the expression of most Fe-regulated genes, except for *NAS4*, which was significantly up-regulated only in the long term (Fig. 7). However, the effect of Co on the expression of these genes was less persistent, as most of them, including *FIT*, *IRT1*, *FRO2*, *FRO3*, and *F6′H1*, were no longer up-regulated after 9 d. Additionally, the expression of ethylene signaling genes remained unaffected by Co as well as by Ni during the whole time course of the experiment.

Despite reducing shoot growth and inducing leaf chlorosis (Fig. 1), an excess of Cd and even more of Ni caused relatively mild changes in the expression patterns of most Fe deficiency-regulated genes (Fig. 7). Nonetheless, both heavy metals were able to enhance transcript levels of *MYB72* as well as of *bHLH100*, *bHLH101*, *bHLH38*, and *bHLH39*, confirming that these genes also are sensitive to Ni and Cd. *PYE*, *BTS*, *EIN3*, *EIL1*, and *FIT* were up-regulated by Cd but not by Ni, even though this response was limited to a single time point (Fig. 7). Interestingly, in spite of the lack of an unequivocal increase in mRNA levels of *FIT*, those of *IRT1* and *FRO2* were induced after 3 d on Ni excess. On the other hand, Ni highly induced the up-regulation of *IDF1*, even though *IRT1* transcript levels of Ni-supplied plants were significantly lower than those measured under Fe deficiency. In the short run, the effect of high Mn doses was restricted to a mild up-regulation of

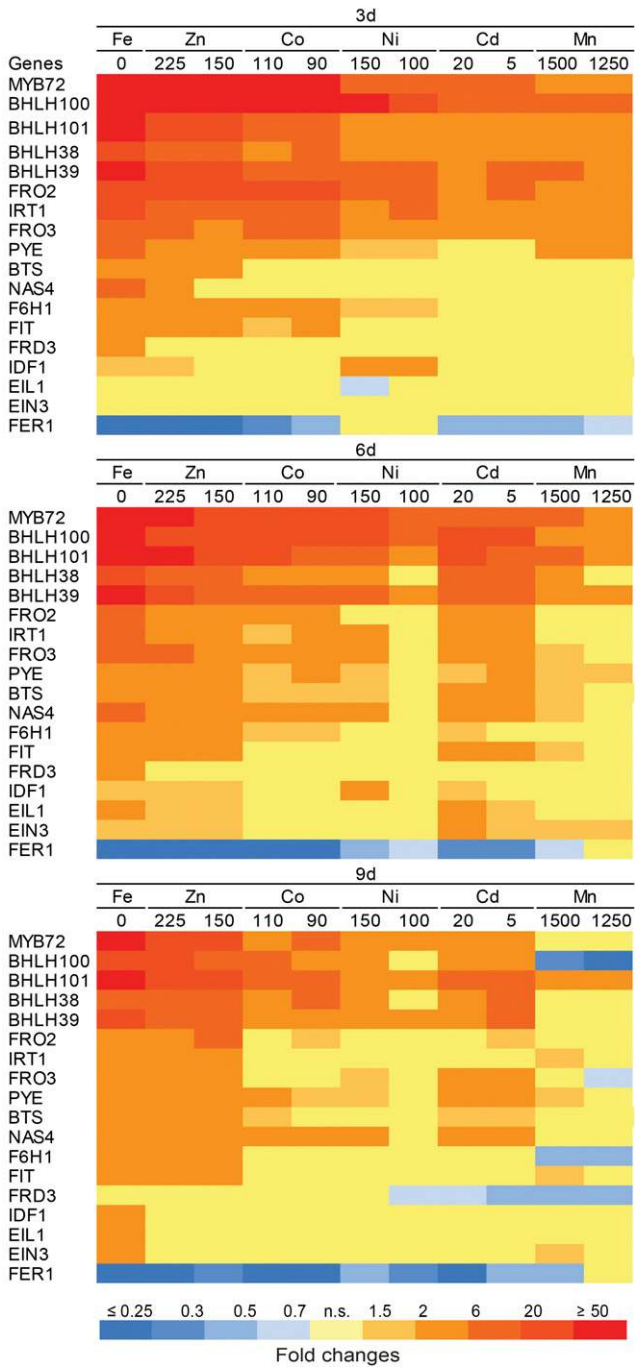

Figure 7. Expression of Fe deficiency-related genes in roots under excess heavy metal supplies. The color code of the heat map indicates a statistically significant ($P < 0.05$) up-regulation (red) or down-regulation (blue) of transcript levels under no supplementation of Fe + 50 μM ferrozine (0 Fe) or under the indicated supplies of heavy metals (μM). Gene expression levels are expressed as fold change from control one-half-strength MS medium treatment supplemented with 75 μm Fe-EDTA. n.s., No statistically significant difference from the control treatment. Plants were precultured for 7 d in one-half-strength MS medium and then transferred to one-half-strength MS medium with (control) or without Fe + 50 μM ferrozine (0 Fe) or with Fe and containing the indicated concentrations of heavy metals (μM) for 3, 6, and 9 d.

IRT1, *FRO2*, *FRO3*, and most Fe-regulated transcription factors, except for *FIT* (Fig. 7). However, after 6 and 9 d of exposure to Mn excess, the expression of most Fe-responsive genes remained at a basal level or was even significantly down-regulated, as was the case for *bHLH100*, *FRD3*, and *F6'H1* after 9 d.

In order to extract major trends of metal-dependent transcriptional responses over time, all transcriptional data obtained in this study were subjected to cluster analysis. As compared with the other heavy metals tested herein, excess Mn produced the most dissimilar transcriptional responses to Fe deficiency (Fig. 8). By contrast, the transcriptional changes induced by Zn excess largely resembled those induced by Fe deficiency. Changes in transcript patterns evoked by elevated Co supplies clustered with low Fe particularly in the short run. Transcriptional changes recorded under Cd and Ni excess resembled to some extent those observed under Fe deficiency only at the intermediate time point (Fig. 8). Taken together, metal-induced transcriptional responses resembled those observed under Fe deficiency in the order Zn > Co > Cd > Ni > Mn.

DISCUSSION

Heavy metal treatments have been frequently reported to mimic Fe deficiency symptoms and to induce Fe deficiency responses in plants (Schaaf et al., 2006; Meda et al., 2007; Fukao et al., 2011; Wu et al., 2012). However, due to a lack of comparability of traits and growth conditions among studies, it remained mostly unclear to what extent individual heavy metals interfere with Fe homeostasis. To address this question, this study took a novel integrative approach by determining shoot and root morphological and physiological traits as well as transcriptional markers from Arabidopsis plants subjected to five heavy metals reported previously to interfere with Fe uptake. Thereby, heavy metal doses were adjusted in a way that leaf chlorosis was induced to a similar extent to that under Fe deficiency. This procedure allowed us to determine which Fe deficiency-related traits are sensitive to heavy metals and to rank metals according to their ability to induce Fe deficiency responses. Our analysis clearly shows that Zn, Co, Cd, and Ni, but not Mn, induce typical Fe deficiency symptoms even before decreasing shoot or root Fe below critical deficiency levels. Notably, these metals strongly differ in the extent, type, and combination of induced Fe deficiency-related responses, indicating that they interfere with Fe homeostasis at distinct levels.

Zn Strongly Induces Fe Deficiency Signaling and Related Physiological Responses

Among all tested metals, elevated Zn supply provoked the strongest induction of Fe deficiency-responsive genes (Figs. 7 and 8) and of typical Fe deficiency-related physiological responses in roots (Figs. 2 and 3). These changes coincided with the growth reduction of roots and shoots as well as with chlorosis in young leaves (Figs. 1 and 4B; Marschner, 2012), although Fe concentrations in shoots and roots were still above 60 μg g^{-1} (Table I; Supplemental Figs. S2 and S3), which are not yet below

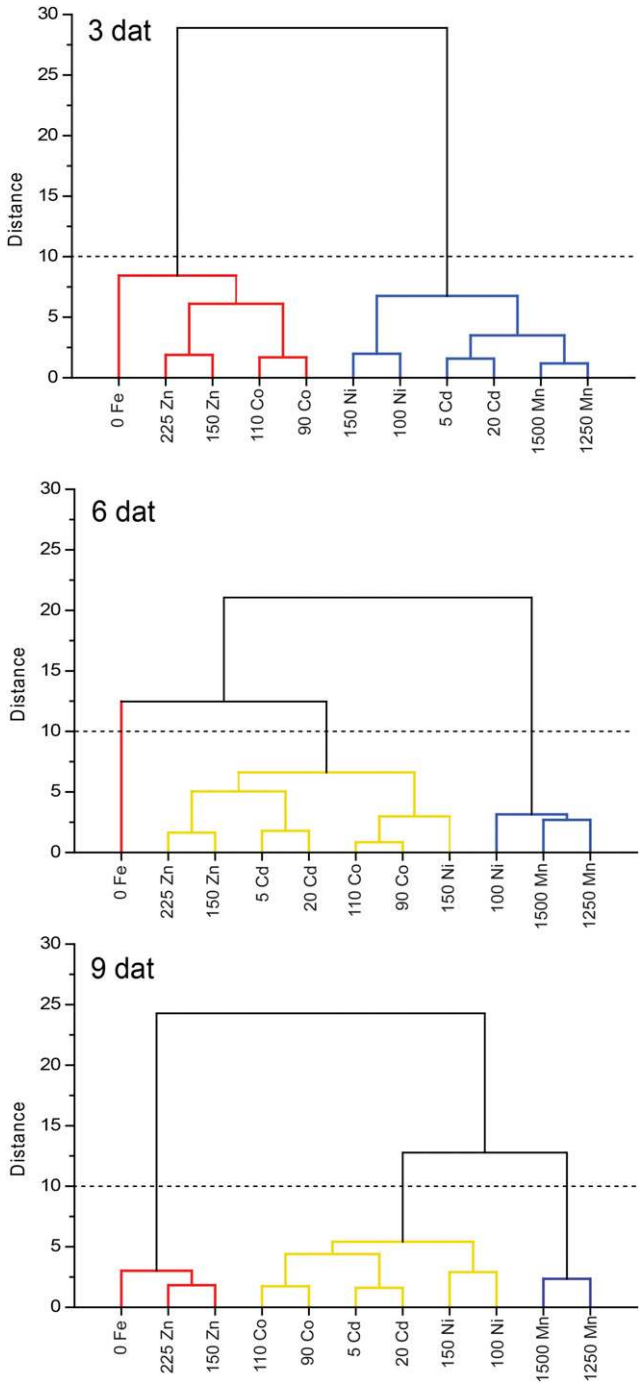

Figure 8. Hierarchical cluster analysis of transcript levels in heavy metal and low-Fe treatments. The dendrogram was obtained by clustering 0 Fe (no Fe + 50 μM ferrozine) and heavy metal treatments based on $\log_2$-transformed values of fold change for each time point separately. The colors of the lines indicate cluster membership. dat, Days after treatment.

the critical deficiency range (Giehl et al., 2012; Marschner, 2012; Gruber et al., 2013). A similar observation was made by Fukao et al. (2011) when excessive Zn reduced chlorophyll levels and induced Fe deficiency stress-responsive proteins, although shoot Fe concentrations remained even above 100 $\mu g\ g^{-1}$. At the root physiological level, the up-regulation of *FRO2* and *F6′H1* expression by excess Zn was translated into a strong stimulation of root FCR activity (Fig. 2B) and an increased synthesis and exudation of coumarins (Fig. 3, B and D). These findings are in accordance with previous studies, which have reported elevated FRO2 protein levels (Fukao et al., 2011) and increased transcript levels of genes coding for enzymes that produce precursors of coumarins under high Zn supply (van de Mortel et al., 2006). Notably, among all heavy metals assessed in this study, Zn induced the strongest root accumulation and release of fluorescent coumarins, although at lower levels than those recorded in Fe-deficient plants (Fig. 3). F6′H1-dependent coumarin synthesis in plants is regulated by FIT and potentially by MYB72 (Schmid et al., 2014; Zamioudis et al., 2014). FIT positively affects the transcript levels of *MYB72*, which regulates the synthesis of several metabolites on the phenylpropanoid pathway, including that of feruloyl-CoA, the precursor of coumarins (Rodríguez-Celma et al., 2013). Since *FIT* and *MYB72* remained up-regulated more consistently by excess Zn than by any other metal (Fig. 7), high Zn mimicked most closely the Fe deficiency response at the molecular and physiological levels.

In terms of RSA, plants from high-Zn treatments resembled those grown under limiting Fe supplies only at lower Zn doses. Not only the phenotypic comparison but, in particular, the multivariate analysis showed that the root architectural traits changed in the same direction in plants treated with either inadequate Fe or elevated Zn concentration (Figs. 4, A and B, and 5; Table II). Furthermore, we showed that foliar Fe supply was able to revert most of the changes in root morphology induced by Zn in wild-type plants (Fig. 6, C and D). Assessing the natural variation in Zn tolerance by a quantitative trait locus mapping approach has revealed that root architectural traits of Arabidopsis plants grown on high Zn are subject to cross talk between mechanisms regulating Fe and Zn homeostasis (Pineau et al., 2012). *FRD3* gene expression and the corresponding citrate-loading activity into the xylem correlated positively with the shoot Fe status and primary root growth when Arabidopsis accessions were grown under high Zn supply. In our experiments, *FRD3* expression was not altered significantly under high Zn (Supplemental Table S2), which may be due to the fact that elevated Zn triggers a complex posttranscriptional regulation of *FRD3* (Charlier et al., 2015). Nevertheless, some effects of Zn surpassed those caused by Fe deficiency, as especially the length of lateral roots was more susceptible to increasing Zn supplies (Figs. 4, A and B, and 5A). Such effects might involve an IRT1-independent uptake pathway, since the lateral root elongation of *irt1* plants by Zn could not be recovered by foliar Fe supply, as opposed to the situation in wild-type plants.

Zn competes with Fe already at the level of uptake via IRT1 (Korshunova et al., 1999) and decreases Fe levels in the roots (Supplemental Fig. S3; Fukao et al., 2011), which, in principle, would be sufficient to explain the subsequent induction of Fe deficiency-related processes. As reported previously (Fukao et al., 2011; Shanmugam et al., 2011, 2012), foliar Fe supply strongly suppressed the development of chlorosis upon excess Zn (Fig. 6, A and B) and reduced shoot Zn accumulation to a certain extent (Supplemental Fig. S5). However, assessing the *irt1* mutant under the same conditions showed that the suppression of Fe deficiency responses under foliar Fe supply was not caused by lower shoot accumulation of Zn (Supplemental Fig. S5). This finding showed that IRT1-mediated Zn uptake was not relevant for the expression of Fe deficiency-related responses but suggested a shoot-derived interaction, in which foliarly supplied Fe outcompeted or displaced Zn from binding sites relevant for shoot-to-root Fe signaling. In agreement with this assumption, we observed in roots that high Zn caused a pronounced and consistent up-regulation of *BTS*, a gene encoding a putative Fe sensor in Arabidopsis (Fig. 7), which might be responsible for the perception of phloem-derived Fe signals in roots (Kobayashi and Nishizawa, 2014). Moreover, we observed that PYE, which is tightly controlled by BTS-mediated Fe deficiency sensing (Selote et al., 2015) and induced by Fe deficiency (Long et al., 2010), also was strongly induced at the transcriptional level by high Zn supply (Fig. 7; Supplemental Table S2). This further supports the view that transcriptional changes observed under excess Zn (Figs. 7 and 8) were caused by an antagonistic interaction between Zn and Fe at the level of Fe sensing and early Fe deficiency signaling, which were then translated into a typical Fe deficiency response.

Co, Cd, and Ni Affect Fe Homeostasis at Distinct Steps

Although Cd, Co, and Ni induced several Fe deficiency-related responses, the effect of each of these heavy metals was less systematic and typically restricted to individual traits. It has been suggested previously that Cd influences Fe-dependent gene regulation at a high hierarchic level (van de Mortel et al., 2008; Hermans et al., 2011). Indeed, high Cd supply resulted in a significant although more transient induction of genes with regulatory functions in Fe homeostasis (Figs. 7 and 8). Among those, *FIT* was less consistently induced than *bHLH38/39* and *bHLH100/101*. In particular, overexpression of *bHLH39* alone, or also of *bHLH38* or *bHLH39* together with *FIT*, have proven efficient in increasing Cd tolerance (Wu et al., 2012), suggesting that Cd modulates the regulation of Fe acquisition genes via bHLH39 rather than via FIT. Despite a moderate induction of *FRO2*, together with *IRT1*, at earlier time points (Figs. 2A and 7), FCR activity in Cd-treated roots remained indistinguishable from that in control roots during the whole course of the experiment (Fig. 2B).

Based on previous studies, there is no consensus about the impact of elevated Cd on FRO2 regulation, as unchanged (Chang et al., 2003), elevated (Chang et al., 2003; Gao et al., 2011), or even repressed (López-Millán et al., 2009; Gao et al., 2011; Hermans et al., 2011) *FRO2* transcription and/or FCR activities have been reported, depending on the Cd concentrations, plant species, or cultivation times used in these studies. However, our study supports the notion that *FRO2* and FCR are not preferential targets of Cd interactions with Fe homeostasis. Instead, Cd showed a prominent induction of *PYE* and its target *NAS4* as well as of *bHLH100/101* (Fig. 7; Supplemental Table S2), indicating that Cd predominantly influences the transcriptional control of genes involved in the long-distance allocation of Fe in plants (Long et al., 2010; Sivitz et al., 2012).

At the root architectural level, elevated Cd supplies induced changes that greatly resembled those of plants suffering from severe Fe deficiency (Figs. 4, A and E, and 5A). However, in particular, primary root length was more inhibited by high Cd than by Fe deficiency (Figs. 4, A and E, and 5A). This may be due to the concomitant decline of Ca concentrations below critical deficiency levels (Table I), which strongly suppresses primary root elongation (Gruber et al., 2013) and may have added to the inhibitory action of Cd itself. This side effect made RSA traits difficult to interpret purely in the light of Cd-Fe interactions.

In the case of Co and Ni, the transcriptional responses evoked by these metals were similar to Fe deficiency at a rather early time point but weaker over the long term (Figs. 7 and 8). High Co and Ni also resulted in a rapid induction of *FRO2* and *F6′H1* expression as well as FCR activity (Figs. 2 and 3A). However, in contrast to Fe deficiency, the expression of *EIN3* and *EIL1* was not altered by excess Co or Ni at any time (Fig. 7). During Fe deficiency, ethylene signaling via EIN3/EIL1 intensifies the response of FIT, FIT-interacting transcription factors, and their downstream elements, as shown by the down-regulation of *FIT*, *IRT1*, *FRO2*, and *bHLH39* in the *ein3eil1* double mutant (Lingam et al., 2011). The ethylene-dependent regulation of these genes also was confirmed by Lucena et al. (2006) and García et al. (2010) by inhibiting ethylene synthesis in Fe-deficient plants with silver thiosulfate or Co supply at levels comparable to those used in our study. Therefore, due to the ability of Co to act as a negative feedback regulator of ethylene synthesis, it is likely that Co suppressed the sustained up-regulation of *FIT* and its target genes in the long run (Figs. 2A, 3A, and 7). By contrast, *PYE* and its target *NAS4* remained induced even after prolonged cultivation under high Co, indicating that the expression of these genes depends less on an ethylene boost (Fig. 7). This scenario may explain the differential regulatory action of Co on FIT- and PYE-dependent gene regulation and support the view of Co affecting Fe acquisition primarily in the short run.

Unlike Zn and Cd treatments, the effect of Ni on the up-regulation of regulatory components was restricted to *bHLHL38*, *bHLHL39*, *MYB72*, *bHLH100*, and *bHLH101* (Fig. 7; Supplemental Table S2). However, it is intriguing that the expression of *IRT1* and *FRO2* (Figs. 2A and 7; Supplemental Table S2) as well as FCR activity (Fig. 2B) were significantly induced by Ni, even in the absence of a clear induction of their closest upstream regulator *FIT*. This observation suggests that the activation of the Fe acquisition machinery by high Ni relies on the activation of other transcription factors, such as bHLH38 and bHLH39. Interestingly, *IDF1* expression was induced in Ni-treated plants to levels comparable to those detected in Fe-deficient plants (Fig. 7). However, *idf1* plants were indistinguishable from wild-type plants when grown under the excess of the heavy metals tested herein (data not shown), suggesting that the degradation of IRT1 through IDF1 neither prevents nor promotes the heavy metal susceptibility of plants. A minor involvement of IRT1 in the induction of Fe deficiency by Ni is reinforced by the finding that not only wild-type plants showed Fe deficiency symptoms but even *irt1* plants developed stronger Fe deficiency-like physiological responses when treated with high Ni (Fig. 6, A, B, and F).

In terms of RSA, Co and especially Ni produced the most distinct changes in relation to the other heavy metals and to Fe deficiency (Figs. 4 and 5). The excess of Co and Ni significantly increased lateral root density, which was opposite to the effect of Fe deficiency or elevated supply of other metals (Fig. 4; Table II). In addition, primary root length was severely inhibited by Ni, while lateral root growth remained unaffected up to higher doses of Ni (Fig. 4D; Table II), indicating that the growth effects on roots of different orders were uncoupled by high Ni supply. Foliar supplementation of Ni-treated plants with Fe was not efficient in reverting the RSA changes, despite the full recovery of chlorosis (Fig. 6, A–E). Thus, distinctive RSA changes induced by Co and especially by Ni were unrelated to Fe deficiency but likely caused by localized toxic effects of these metals.

Excess Mn Provokes Fe Deficiency in the Absence of IRT1

In wild-type plants, excess Mn evoked changes in RSA that strongly resembled Fe deficiency (Figs. 4, A and F, and 5A). However, respecting the weak interaction of Fe and Mn at the regulatory and physiological levels (Figs. 1–3, 7, and 8), it is less likely that the morphological root phenotype was a consequence of Mn-induced Fe deficiency in roots. This assumption was additionally reinforced by the fact that extra Fe supply did not alter Mn-dependent root architectural traits (Fig. 6, C–E). The root phenotype provoked by excess Mn also can hardly be explained by the recorded Ca and Mg deficiency (Table I), as either of the related root phenotypes showed a different coupling of affected root traits (Gruber et al., 2013). In this regard, it has been shown that primary root elongation is more sensitive to Mn deficiency than lateral root branching or elongation (Gruber et al., 2013). Together with the observation that primary root elongation was less

sensitive to excess Mn than lateral root branching and elongation (Fig. 4F; Table II), this may suggest a higher Mn requirement for primary root elongation than for lateral root development. Thus, it is more likely that excess Mn shaped RSA in a similar way to Fe deficiency did by directly affecting the root developmental program.

Mn serves as a substrate for IRT1, and thus, Mn and Fe competition can already take place at the level of root uptake (Vert et al., 2002). Unlike the other metals assessed herein, the effect of Mn on Fe deficiency responses was very limited and restricted mainly to responses at the root level. In shoots, exposure of plants to Mn neither induced chlorosis in young leaves (Fig. 1, A and B) nor substantially reduced Fe levels (Table I). Even when considerably higher Mn concentrations were supplied to plants, which resulted in severely stunted shoot and root growth and the appearance of brown spots on leaves, no signs of chlorosis were observed in wild-type plants (Supplemental Fig. S1). In fact, the formation of brown spots on leaves upon high Mn supply results from Mn deposition in the leaf apoplast, which might prevent intracellular interference of this heavy metal with Fe homeostasis (Fecht-Christoffers et al., 2006). Intriguingly, decreased chlorophyll concentrations or the appearance of pale/yellowish color in leaves have been reported as long-term symptoms of excess Mn supply in cowpea (*Vigna unguiculata*; Horst, 1983), wheat (*Triticum aestivum*; Moroni et al., 1991), or even Arabidopsis (Dixit and Dhankher, 2011). However, in these studies, Mn-induced chlorosis was not restricted to young leaves, as is most typical for Fe deficiency (Vert et al., 2002; Schmid et al., 2014). Notably, in our experiments, excess Mn decreased the concentrations of Ca and especially of Mg (Table I) below critical deficiency levels for Arabidopsis plants (Gruber et al., 2013). Therefore, excess Mn interferes more significantly with Mg or even Ca nutrition than with Fe. In fact, we found that, upon prolonged Mn exposure, almost none of the Fe deficiency-induced genes were induced anymore, and several genes related to Fe acquisition, such as *F6′H1*, or Fe allocation, such as *bHLH100* and *FRD3*, were even down-regulated (Fig. 7). Nevertheless, high Mn supply decreased Fe levels in the roots (Supplemental Fig. S3), down-regulated the expression of *FER1*, and caused a slight, short-term up-regulation of genes with regulatory functions in Fe acquisition or distribution (Figs. 2A and 7; Supplemental Table S2). Excess Mn led only initially to a slight induction of *FRO2* gene expression and root FCR activity (Fig. 2), indicating that other Fe-related root physiological responses were sufficient to cope with an enhanced Mn over Fe uptake. In this context, a critical component preventing cytosolic Mn overload in Fe-deficient Arabidopsis plants turned out to be MTP8 (Eroglu et al., 2016). *MTP8* gene expression is under the control of FIT, and the corresponding protein is responsible for Mn loading into root vacuoles. Hence, *mtp8* mutants suffer from Fe deficiency in the presence of Mn (Eroglu et al., 2016). Likewise, *irt1* mutant plants developed severe symptoms of Fe deficiency upon high Mn supply, as revealed by the appearance of chlorosis and the strong increase of FCR activity (Fig. 6, A, B, and F). A similar scenario can be observed when wild-type plants are cultivated under low-Fe and high-Mn conditions (Eroglu et al., 2016). This suggests that, once Fe deficiency responses are induced, the presence of additional Mn can even strengthen the severity of the symptoms. Our study also revealed that the promotion of Fe deficiency responses by Mn does not rely on IRT1-mediated uptake. Instead, uptake by IRT1 circumvents the interactions between Mn and Fe. It is possible that other unspecific metal transporters, highly expressed under low external Fe concentrations and derepressed in the absence of IRT1, are responsible for Mn-induced Fe deficiency. The most likely candidate appears to be NRAMP1, which facilitates the uptake not only of Mn but also of Fe (Cailliatte et al., 2010; Castaings et al., 2016).

CONCLUSION

Even though elevated supplies of Zn, Co, Ni, and Cd caused typical symptoms of Fe deficiency-induced chlorosis and reduced shoot or root Fe levels to a similar extent that remained above critical deficiency levels, each metal elicited a different set of Fe deficiency-related responses. Among all tested metals,

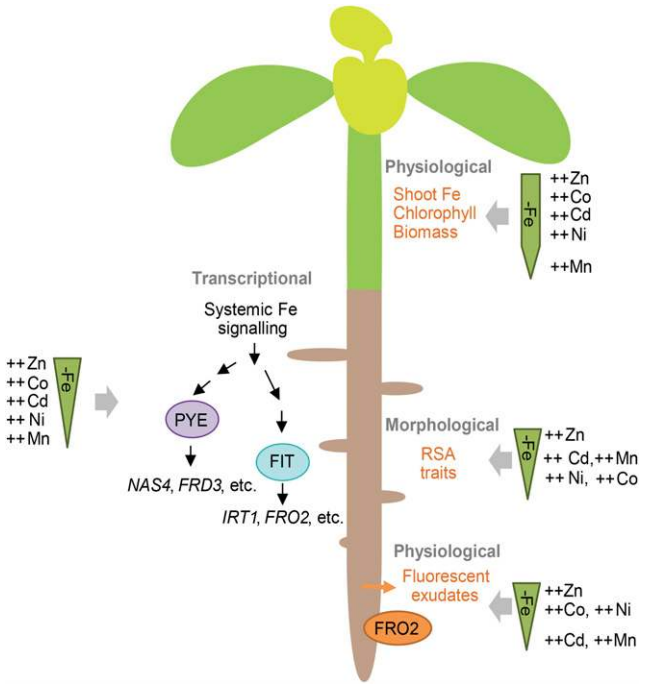

Figure 9. Fe deficiency response scheme highlighting the relative impact of individual heavy metals on Fe deficiency-induced processes in Arabidopsis. The ranking of metals along the geometrical forms represents their degree of interference with Fe deficiency responses at the shoot or root physiological, morphological, or transcriptional level. Details are described in the text.

excess Zn supply mimicked Fe deficiency the most, as expressed by a strong induction of the Fe-dependent regulatory gene network and its related downstream physiological as well as early morphological responses in roots (Fig. 9). Thus, an impaired balance between Fe and Zn appears to be perceived as Fe deficiency at the regulatory level, where the sensing of systemic Fe deficiency takes place. Co, Ni, or Cd evoke selective or transient responses resembling those of Fe deficiency. Although high Ni up-regulates the expression of a limited number of Fe-related transcription factors, this induction is sufficient for a pronounced physiological response in roots (Fig. 9). The effect of Co and, to a lesser extent, Ni is characterized by an early and transient stimulation of root physiological processes, likely due to a lack of induction of the ethylene-dependent response pathway. Both Ni and Co increase lateral root density and, thus, affect root morphology in a dissimilar way to Fe deficiency. This differential effect strongly argues in favor of an uncoupled interference of these metals on Fe deficiency responses at the physiological and morphological levels. Although Cd-induced leaf symptoms resemble Fe deficiency, Cd induces rather inconsistent changes in Fe-related physiological, morphological, or molecular responses in roots, which may be due to negative Cd-Fe interactions at a lower hierarchic level (e.g. during transport or metabolism). Among all tested metals, Mn is the weakest inducer of regulatory and physiological responses typical for Fe deficiency in wild-type plants (Fig. 9). However, Mn intensifies Fe deficiency responses if specific transporters are lacking, such as IRT1 or MTP8. Thus, we conclude that the induction of Fe deficiency responses by the investigated heavy metals takes place at different regulatory and mechanistic levels and that metal-induced physiological and morphological processes mimicking Fe deficiency are uncoupled.

MATERIALS AND METHODS

Plant Material and Growth Conditions

The accession line Col-0 of Arabidopsis (*Arabidopsis thaliana*) was used in this study unless indicated otherwise. The *irt1* mutant (Col-0 background) has been characterized by Varotto et al. (2002). Seeds were surface sterilized with 70% (v/v) ethanol and 0.05% (v/v) Triton X-100. The seeds were sown on preculture medium consisting of one-half-strength MS medium (Murashige and Skoog, 1962) with 75 μM Fe-EDTA, 0.5% (w/v) Suc, and 1% Difco agar (Becton Dickinson). The pH of the medium was kept at 5.5 by adding 2.5 mM MES buffer adjusted to pH 5.5. The agar plates containing the seeds were kept for 48 h in 4°C. Afterward, the plates were placed vertically inside growth cabinets and precultured under a regime of 10 h of light (120 μmol m^{-2} s^{-1}, 22°C) and 14 h of dark (19°C) for 7 d. Seedlings were then transferred to fresh agar plates of different composition depending on the experiment. Control plants were cultivated under one-half-strength MS conditions with 75 μM Fe(III)-EDTA, unless stated otherwise, whereas Fe deficiency was obtained as indicated. In some cases, Fe deficiency was induced by supplying no Fe plus 50 μM ferrozine [3-(2-pyridyl)-5,6-diphenyl-1,2,4-triazine sulfonate; Serva]. Heavy metals were added to one-half-strength MS medium as $ZnSO_4O \cdot 7H_2O$, $CoCl_2O \cdot 6H_2O$, $NiSO_4 \cdot 6H_2O$, $CdCl_2 \cdot H_2O$, or $MnSO_4 \cdot H_2O$ salts to obtain the concentrations indicated in the figure legends. For experiments with foliar Fe supply, Fe was provided as ammonium ferric citrate. In these experiments, the agar was separated horizontally into two segments and shoots were placed on the top segment to avoid diffusion of the foliar supplied Fe solution into the bottom, root-containing segment.

RSA and PCA

After 10 d of cultivation on treatments, plants were scanned with an Epson Expression 10000XL scanner (Seiko Epson) at a resolution of 300 dots per inch using settings described by Gruber et al. (2013). Primary root lengths, total lateral root lengths, and lateral root numbers from 30 to 40 plants per treatment were analyzed using WinRhizo Pro version 2009c (Reagent Instrument). Average lateral root length was calculated by dividing the total length of lateral roots by the number of lateral roots. The density of the lateral roots was calculated by dividing the number of lateral roots by the length of the primary root.

PCA was performed on independent root traits, namely primary root length, average lateral root length, and lateral root density, from all treatments. Prior to analysis, root trait data were normalized using a modified z-score normalization algorithm (Gruber et al., 2013):

$$\tilde{X} = \frac{X - \mu^{1/2\text{MS control treatment}}}{\sigma^{1/2\text{MS control treatment}} / \sigma^{\text{allcontrols}}} + \mu^{\text{allcontrols}}$$

where $\mu^{1/2\text{MS control treatment}}$ and $\sigma^{1/2\text{MS control treatment}}$ are the observed mean and SD of the control one-half-strength MS treatment in any given experiment and $\sigma^{\text{all controls}}$ and $\mu^{\text{all controls}}$ are the global mean and SD calculated from the control one-half-strength MS treatments across all experiments.

The normalized root trait values were used as input data for PCA performed with the R package ADE-4 (Thioulouse et al., 1997). For better visibility, the distribution of control treatments is magnified in Supplemental Figure S7. The first two components, which explained 93% of the total variability in RSA, were correlated with the normalized root trait data, and coefficients of determination were calculated.

The statistical significance among treatments was tested with Student's *t* test or Tukey's test for two-group and ANOVA-based multiple group comparisons, respectively. The statistical tests were undertaken with SigmaPlot version 11.0 (Systat Software).

Chlorophyll and Element Analyses

Depending on the experiment, whole shoots were harvested or old and young leaves were collected separately before weighing. Chlorophyll was extracted by incubating whole shoots in *N*,*N*′-dimethylformamide (Merck) for 48 h at 4°C. The absorbance of the extract was measured at 647 and 664 nm, and total chlorophyll concentrations were calculated using the formula described by Moran (1982).

The removal of metals from the root apoplast was achieved by washing roots as described previously (Cailliatte et al., 2010; Zhai et al., 2014). Briefly, roots were washed in 2 mM $CaSO_4$ and 10 mM EDTA for 10 min followed by washing in a solution containing 0.3 mM bathophenanthroline disulfonate and 5.7 mM sodium dithionite for 3 min. Roots were then rinsed three times with deionized water.

Root and shoot samples were dried at 65°C and digested with HNO_3 in polytetrafluoroethylene tubes and in a pressurized system (UltraCLAVE IV; MLS). Elemental analysis of whole shoots was performed by inductively coupled plasma-optical emission spectrometry (iCAP 6500 Dual OES Spectrometer; Thermo Fisher Scientific), whereas young leaves, old leaves, and roots were analyzed by sector field high-resolution inductively coupled plasma-mass spectrometry (ELEMENT 2; Thermo Fisher Scientific). In both cases, element standards were prepared from certified reference materials from CPI International.

Ferric-Chelate Reductase Activity and Detection of Fluorescent Compounds in Roots

Root ferric-chelate reductase activity was determined by placing the roots of plants previously cultivated for 3, 6, or 9 d on treatments into a mixture of 0.1 mM Fe(III)-EDTA, 0.2 mM $CaSO_4$, 5 mM MES, pH 5.5, and 0.2 mM ferrozine (Waters et al., 2006). The formation of pink coloration, indicative for Fe(II)-ferrozine complexes, was monitored over time. The reaction was stopped after 90 to 120 min, plants were removed from the solution, and roots were cut and weighed. An aliquot of the stained solution was removed, and the absorbance was measured at 562 nm. The concentration of Fe(II)-ferrozine complexes was calculated using 28.6 mmol dm^{-3} cm^{-1} as molar extinction coefficient (Yi and Guerinot, 1996).

Prior to fluorescence visualization, plants were exposed to UV radiation at 365 nm using a 20-ms exposure time. The emitted root and agar fluorescence was captured by the fluorescence imaging system Quantum ST4 (Vilber Lourmat) equipped with a 440-nm filter (F-440M58). Root fluorescence measurements were taken from equal lengths of the subapical parts of the roots, where most of the fluorescence accumulated. Agar fluorescence measurements were recorded from equal areas and distances from the roots, and average pixel intensities were used as relative quantification units of fluorescence. For background correction, average pixel intensities of the empty bottom parts of the agar were used. Image analysis was undertaken by ImageJ software.

Gene Expression and Cluster Analyses

Total RNA of the roots was extracted using the Trizol method (Invitrogen) according to the manufacturer's instructions. Samples were treated with DNase to remove all potential DNA contamination. cDNA was synthesized by reverse transcription of the RNA using the RevertAid First Strand cDNA Synthesis Kit of Fermentas and oligo(dT) primer. Mastercycler epgradient S realplex^2 (Eppendorf) was used to carry out quantitative real-time PCR on cDNA templates and iQ SYBR Green Supermix (Bio-Rad Laboratories) mixture. Three reference genes, namely *UBQ2*, *SAND family protein*, and *F-Box protein*, previously used in Fe deficiency- or heavy metal-related studies, were tested for gene expression stability (Remans et al., 2008; Schmid et al., 2014). Gene expression stability was inspected with RefFinder (http://150.216.56.64/referencegene.php), a Web-based tool that integrates the currently available major computational programs (geNorm, Normfinder, BestKeeper, and the comparative ΔC_t method) to compare and rank the tested reference genes (Llanos et al., 2015). *UBQ2* showed the highest stability; therefore, this reference gene was used in all expression analyses to normalize gene expression levels of the target genes (Supplemental Fig. S6). Gene expression levels were expressed as fold changes from control one-half-strength MS treatment using the following equation (Pfaffl, 2004):

$$\text{Fold change} = \frac{E_{\text{target gene}}^{\Delta C_t \text{target gene(control-sample)}}}{E_{\text{reference gene}}^{\Delta C_t \text{reference gene(control-sample)}}}$$

where E is gene amplification efficiency derived from the standard curve and C_t is cycle threshold. All primers used in the quantitative real-time PCR are listed in Supplemental Table S3.

Fold change values were $\log_2$ transformed in order to correct for heteroscedasticity in the data set (van den Berg et al., 2006). These transformed values then served as input data for hierarchical cluster analysis of treatments conducted for each time point separately. Cluster analysis was performed with R software using Ward's method and Euclidean distance.

Supplemental Data

The following supplemental materials are available.

Supplemental Figure S1. Effects of strongly elevated Mn supply on leaf symptoms and shoot fresh weight.

Supplemental Figure S2. Metal concentrations in young and old leaves of Arabidopsis (Col-0).

Supplemental Figure S3. Metal concentrations in roots of Arabidopsis (Col-0) plants.

Supplemental Figure S4. Impact of the Fe source on the development of heavy metal-induced Fe deficiency responses.

Supplemental Figure S5. Effects of foliar Fe supply on shoot metal concentrations in Col-0 and *irt1* plants.

Supplemental Figure S6. Distribution of C_t values of reference genes tested for expression stability.

Supplemental Figure S7. PCA of the variation in RSA traits in control treatments for all heavy metal treatments.

Supplemental Table S1. Relative proportions of individual Fe species in metal-supplemented cultivation medium.

Supplemental Table S2. Effects of low Fe and high heavy metal supply on transcript levels of genes involved in Fe deficiency-related responses.

Supplemental Table S3. List of primers used in the study.

ACKNOWLEDGMENTS

We thank Susanne Reiner and Yudelsy A. Tandron Moya for excellent technical assistance with elemental analysis.

Received December 19, 2016; accepted May 4, 2017; published May 12, 2017.

LITERATURE CITED

Allen MD, Kropat J, Tottey S, Del Campo JA, Merchant SS (2007) Manganese deficiency in Chlamydomonas results in loss of photosystem II and MnSOD function, sensitivity to peroxides, and secondary phosphorus and iron deficiency. Plant Physiol **143:** 263–277

Becher M, Talke IN, Krall L, Krämer U (2004) Cross-species microarray transcript profiling reveals high constitutive expression of metal homeostasis genes in shoots of the zinc hyperaccumulator *Arabidopsis halleri*. Plant J **37:** 251–268

Besson-Bard A, Gravot A, Richaud P, Auroy P, Duc C, Gaymard F, Taconnat L, Renou JP, Pugin A, Wendehenne D (2009) Nitric oxide contributes to cadmium toxicity in Arabidopsis by promoting cadmium accumulation in roots and by up-regulating genes related to iron uptake. Plant Physiol **149:** 1302–1315

Briat JF, Ravet K, Arnaud N, Duc C, Boucherez J, Touraine B, Cellier F, Gaymard F (2010) New insights into ferritin synthesis and function highlight a link between iron homeostasis and oxidative stress in plants. Ann Bot (Lond) **105:** 811–822

Cailliatte R, Schikora A, Briat JF, Mari S, Curie C (2010) High-affinity manganese uptake by the metal transporter NRAMP1 is essential for *Arabidopsis* growth in low manganese conditions. Plant Cell **22:** 904–917

Castaings L, Caquot A, Loubet S, Curie C (2016) The high-affinity metal transporters NRAMP1 and IRT1 team up to take up iron under sufficient metal provision. Sci Rep **6:** 37222

Chang YC, Zouari M, Gogorcena Y, Lucena JJ, Abadía J (2003) Effects of cadmium and lead on ferric chelate reductase activities in sugar beet roots. Plant Physiol Biochem **41:** 999–1005

Charlier JB, Polese C, Nouet C, Carnol M, Bosman B, Krämer U, Motte P, Hanikenne M (2015) Zinc triggers a complex transcriptional and post-transcriptional regulation of the metal homeostasis gene FRD3 in Arabidopsis relatives. J Exp Bot **66:** 3865–3878

Colangelo EP, Guerinot ML (2004) The essential basic helix-loop-helix protein FIT1 is required for the iron deficiency response. Plant Cell **16:** 3400–3412

Connolly EL, Campbell NH, Grotz N, Prichard CL, Guerinot ML (2003) Overexpression of the FRO2 ferric chelate reductase confers tolerance to growth on low iron and uncovers posttranscriptional control. Plant Physiol **133:** 1102–1110

Connolly EL, Fett JP, Guerinot ML (2002) Expression of the IRT1 metal transporter is controlled by metals at the levels of transcript and protein accumulation. Plant Cell **14:** 1347–1357

Dixit AR, Dhankher OP (2011) A novel stress-associated protein 'AtSAP10' from *Arabidopsis thaliana* confers tolerance to nickel, manganese, zinc, and high temperature stress. PLoS ONE **6:** e20921

Durrett TP, Gassmann W, Rogers EE (2007) The FRD3-mediated efflux of citrate into the root vasculature is necessary for efficient iron translocation. Plant Physiol **144:** 197–205

Eroglu S, Meier B, von Wirén N, Peiter E (2016) The vacuolar manganese transporter MTP8 determines tolerance to iron deficiency-induced chlorosis in Arabidopsis. Plant Physiol **170:** 1030–1045

Fecht-Christoffers MM, Führs H, Braun HP, Horst WJ (2006) The role of hydrogen peroxide-producing and hydrogen peroxide-consuming peroxidases in the leaf apoplast of cowpea in manganese tolerance. Plant Physiol **140:** 1451–1463

Fourcroy P, Sisó-Terraza P, Sudre D, Savirón M, Reyt G, Gaymard F, Abadía A, Abadía J, Alvarez-Fernández A, Briat JF (2014) Involvement of the ABCG37 transporter in secretion of scopoletin and derivatives by Arabidopsis roots in response to iron deficiency. New Phytol **201:** 155–167

Fukao Y, Ferjani A, Tomioka R, Nagasaki N, Kurata R, Nishimori Y, Fujiwara M, Maeshima M (2011) iTRAQ analysis reveals mechanisms of growth defects due to excess zinc in Arabidopsis. Plant Physiol **155:** 1893–1907

Gao C, Wang Y, Xiao DS, Qiu CP, Han DG, Zhang XZ, Wu T, Han ZH (2011) Comparison of cadmium-induced iron-deficiency responses and

genuine iron-deficiency responses in *Malus xiaojinensis*. Plant Sci **181:** 269–274

García MJ, Lucena C, Romera FJ, Alcántara E, Pérez-Vicente R (2010) Ethylene and nitric oxide involvement in the up-regulation of key genes related to iron acquisition and homeostasis in Arabidopsis. J Exp Bot **61:** 3885–3899

Giehl RFH, Gruber BD, von Wirén N (2014) It's time to make changes: modulation of root system architecture by nutrient signals. J Exp Bot **65:** 769–778

Giehl RFH, Lima JE, von Wirén N (2012) Localized iron supply triggers lateral root elongation in *Arabidopsis* by altering the AUX1-mediated auxin distribution. Plant Cell **24:** 33–49

Giehl RFH, Meda AR, von Wirén N (2009) Moving up, down, and everywhere: signaling of micronutrients in plants. Curr Opin Plant Biol **12:** 320–327

Gruber BD, Giehl RFH, Friedel S, von Wirén N (2013) Plasticity of the Arabidopsis root system under nutrient deficiencies. Plant Physiol **163:** 161–179

Gustafsson JP (2012) Visual MINTEQ version 3.0. http://vminteq.lwr.kth.se

Henriques R, Jásik J, Klein M, Martinoia E, Feller U, Schell J, Pais MS, Koncz C (2002) Knock-out of Arabidopsis metal transporter gene IRT1 results in iron deficiency accompanied by cell differentiation defects. Plant Mol Biol **50:** 587–597

Hermans C, Chen J, Coppens F, Inzé D, Verbruggen N (2011) Low magnesium status in plants enhances tolerance to cadmium exposure. New Phytol **192:** 428–436

Horst WJ (1983) Factors responsible for genotypic manganese tolerance in cowpea (*Vigna unguiculata*). Plant Soil **72:** 213–218

Jain A, Sinilal B, Dhandapani G, Meagher RB, Sahi SV (2013) Effects of deficiency and excess of zinc on morphophysiological traits and spatiotemporal regulation of zinc-responsive genes reveal incidence of cross talk between micro- and macronutrients. Environ Sci Technol **47:** 5327–5335

Kobayashi T, Nagasaka S, Senoura T, Itai RN, Nakanishi H, Nishizawa NK (2013) Iron-binding haemerythrin RING ubiquitin ligases regulate plant iron responses and accumulation. Nat Commun **4:** 2792

Kobayashi T, Nishizawa NK (2014) Iron sensors and signals in response to iron deficiency. Plant Sci **224:** 36–43

Korshunova YO, Eide D, Clark WG, Guerinot ML, Pakrasi HB (1999) The IRT1 protein from *Arabidopsis thaliana* is a metal transporter with a broad substrate range. Plant Mol Biol **40:** 37–44

Lanquar V, Ramos MS, Lelièvre F, Barbier-Brygoo H, Krieger-Liszkay A, Krämer U, Thomine S (2010) Export of vacuolar manganese by AtNRAMP3 and AtNRAMP4 is required for optimal photosynthesis and growth under manganese deficiency. Plant Physiol **152:** 1986–1999

Lequeux H, Hermans C, Lutts S, Verbruggen N (2010) Response to copper excess in *Arabidopsis thaliana*: impact on the root system architecture, hormone distribution, lignin accumulation and mineral profile. Plant Physiol Biochem **48:** 673–682

Lingam S, Mohrbacher J, Brumbarova T, Potuschak T, Fink-Straube C, Blondet E, Genschik P, Bauer P (2011) Interaction between the bHLH transcription factor FIT and ETHYLENE INSENSITIVE3/ETHYLENE INSENSITIVE3-LIKE1 reveals molecular linkage between the regulation of iron acquisition and ethylene signaling in *Arabidopsis*. Plant Cell **23:** 1815–1829

Llanos A, François JM, Parrou JL (2015) Tracking the best reference genes for RT-qPCR data normalization in filamentous fungi. BMC Genomics **16:** 71

Long TA, Tsukagoshi H, Busch W, Lahner B, Salt DE, Benfey PN (2010) The bHLH transcription factor POPEYE regulates response to iron deficiency in *Arabidopsis* roots. Plant Cell **22:** 2219–2236

López-Millán AF, Sagardoy R, Solanas M, Abadía A, Abadía J (2009) Cadmium toxicity in tomato (*Lycopersicon esculentum*) plants grown in hydroponics. Environ Exp Bot **65:** 376–385

Lucena C, Waters BM, Romera FJ, García MJ, Morales M, Alcántara E, Pérez-Vicente R (2006) Ethylene could influence ferric reductase, iron transporter, and H^+-ATPase gene expression by affecting FER (or FER-like) gene activity. J Exp Bot **57:** 4145–4154

Malamy JE (2005) Intrinsic and environmental response pathways that regulate root system architecture. Plant Cell Environ **28:** 67–77

Marschner P (2012) Marschner's Mineral Nutrition of Higher Plants, Ed 3. Academic Press, San Diego, CA

Meda AR, Scheuermann EB, Prechsl UE, Erenoglu B, Schaaf G, Hayen H, Weber G, von Wirén N (2007) Iron acquisition by phytosiderophores contributes to cadmium tolerance. Plant Physiol **143:** 1761–1773

Moran R (1982) Formulae for determination of chlorophyllous pigments extracted with N,N-dimethylformamide. Plant Physiol **69:** 1376–1381

Moroni JS, Briggs KG, Taylor GJ (1991) Chlorophyll content and leaf elongation rate in wheat seedlings as a measure of manganese tolerance. Plant Soil **136:** 1–9

Morrissey J, Baxter IR, Lee J, Li L, Lahner B, Grotz N, Kaplan J, Salt DE, Guerinot ML (2009) The ferroportin metal efflux proteins function in iron and cobalt homeostasis in *Arabidopsis*. Plant Cell **21:** 3326–3338

Murashige T, Skoog F (1962) A revised medium for rapid growth and bio assays with tobacco tissue cultures. Physiol Plant **15:** 473–497

Nagajyoti P, Lee K, Sreekanth T (2010) Heavy metals, occurrence and toxicity for plants: a review. Environ Chem Lett **8:** 199–216

Nishida S, Tsuzuki C, Kato A, Aisu A, Yoshida J, Mizuno T (2011) AtIRT1, the primary iron uptake transporter in the root, mediates excess nickel accumulation in *Arabidopsis thaliana*. Plant Cell Physiol **52:** 1433–1442

Palmer CM, Hindt MN, Schmidt H, Clemens S, Guerinot ML (2013) MYB10 and MYB72 are required for growth under iron-limiting conditions. PLoS Genet **9:** e1003953

Pfaffl MW (2004) A-Z of Quantitative PCR. International University Line, La Jolla, CA

Pineau C, Loubet S, Lefoulon C, Chalies C, Fizames C, Lacombe B, Ferrand M, Loudet O, Berthomieu P, Richard O (2012) Natural variation at the FRD3 MATE transporter locus reveals cross-talk between Fe homeostasis and Zn tolerance in *Arabidopsis thaliana*. PLoS Genet **8:** e1003120

Remans T, Smeets K, Opdenakker K, Mathijsen D, Vangronsveld J, Cuypers A (2008) Normalisation of real-time RT-PCR gene expression measurements in *Arabidopsis thaliana* exposed to increased metal concentrations. Planta **227:** 1343–1349

Reyt G, Boudouf S, Boucherez J, Gaymard F, Briat JF (2015) Iron- and ferritin-dependent reactive oxygen species distribution: impact on Arabidopsis root system architecture. Mol Plant **8:** 439–453

Richard O, Pineau C, Loubet S, Chalies C, Vile D, Marquès L, Berthomieu P (2011) Diversity analysis of the response to Zn within the *Arabidopsis thaliana* species revealed a low contribution of Zn translocation to Zn tolerance and a new role for Zn in lateral root development. Plant Cell Environ **34:** 1065–1078

Robinson NJ, Procter CM, Connolly EL, Guerinot ML (1999) A ferric-chelate reductase for iron uptake from soils. Nature **397:** 694–697

Rodríguez-Celma J, Lin WD, Fu GM, Abadía J, López-Millán AF, Schmidt W (2013) Mutually exclusive alterations in secondary metabolism are critical for the uptake of insoluble iron compounds by Arabidopsis and *Medicago truncatula*. Plant Physiol **162:** 1473–1485

Schaaf G, Honsbein A, Meda AR, Kirchner S, Wipf D, von Wirén N (2006) AtIREG2 encodes a tonoplast transport protein involved in iron-dependent nickel detoxification in *Arabidopsis thaliana* roots. J Biol Chem **281:** 25532–25540

Schmid NB, Giehl RFH, Döll S, Mock HP, Strehmel N, Scheel D, Kong X, Hider RC, von Wirén N (2014) Feruloyl-CoA 6′-Hydroxylase1-dependent coumarins mediate iron acquisition from alkaline substrates in Arabidopsis. Plant Physiol **164:** 160–172

Schmidt H, Günther C, Weber M, Spörlein C, Loscher S, Böttcher C, Schobert R, Clemens S (2014) Metabolome analysis of *Arabidopsis thaliana* roots identifies a key metabolic pathway for iron acquisition. PLoS ONE **9:** e102444

Selote D, Samira R, Matthiadis A, Gillikin JW, Long TA (2015) Iron-binding E3 ligase mediates iron response in plants by targeting basic helix-loop-helix transcription factors. Plant Physiol **167:** 273–286

Shahid M, Pourrut B, Dumat C, Nadeem M, Aslam M, Pinelli E (2014) Heavy-metal-induced reactive oxygen species: phytotoxicity and physicochemical changes in plants. Rev Environ Contam Toxicol **232:** 1–44

Shanmugam V, Lo JC, Wu CL, Wang SL, Lai CC, Connolly EL, Huang J-L, Yeh KC (2011) Differential expression and regulation of iron-regulated metal transporters in *Arabidopsis halleri* and *Arabidopsis thaliana*: the role in zinc tolerance. New Phytol **190:** 125–137

Shanmugam V, Tsednee M, Yeh KC (2012) ZINC TOLERANCE INDUCED BY IRON 1 reveals the importance of glutathione in the cross-homeostasis between zinc and iron in *Arabidopsis thaliana*. Plant J **69:** 1006–1017

Shin LJ, Lo JC, Chen GH, Callis J, Fu H, Yeh KC (2013) IRT1 degradation factor1, a ring E3 ubiquitin ligase, regulates the degradation of iron-regulated transporter1 in *Arabidopsis*. Plant Cell **25:** 3039–3051

Sivitz AB, Hermand V, Curie C, Vert G (2012) Arabidopsis bHLH100 and bHLH101 control iron homeostasis via a FIT-independent pathway. PLoS ONE **7:** e44843

Smith RM, Martell AE (1989) Critical Stability Constants, **Vol 6**. Plenum Press, New York

Solti A, Gáspár L, Mészáros I, Szigeti Z, Lévai L, Sárvári E (2008) Impact of iron supply on the kinetics of recovery of photosynthesis in Cd-stressed poplar (*Populus glauca*). Ann Bot (Lond) **102:** 771–782

Thioulouse J, Chessel D, Doledec S, Olivier JM (1997) ADE-4: a multivariate analysis and graphical display software. Stat Comput **7:** 75–83

van de Mortel JE, Almar Villanueva L, Schat H, Kwekkeboom J, Coughlan S, Moerland PD, Ver Loren van Themaat E, Koornneef M, Aarts MGM (2006) Large expression differences in genes for iron and zinc homeostasis, stress response, and lignin biosynthesis distinguish roots of *Arabidopsis thaliana* and the related metal hyperaccumulator *Thlaspi caerulescens*. Plant Physiol **142:** 1127–1147

van de Mortel JE, Schat H, Moerland PD, Ver Loren van Themaat E, van der Ent S, Blankestijn H, Ghandilyan A, Tsiatsiani S, Aarts MGM (2008) Expression differences for genes involved in lignin, glutathione and sulphate metabolism in response to cadmium in *Arabidopsis thaliana* and the related Zn/Cd-hyperaccumulator *Thlaspi caerulescens*. Plant Cell Environ **31:** 301–324

van den Berg RA, Hoefsloot HCJ, Westerhuis JA, Smilde AK, van der Werf MJ (2006) Centering, scaling, and transformations: improving the biological information content of metabolomics data. BMC Genomics **7:** 142

Varotto C, Maiwald D, Pesaresi P, Jahns P, Salamini F, Leister D (2002) The metal ion transporter IRT1 is necessary for iron homeostasis and efficient photosynthesis in *Arabidopsis thaliana*. Plant J **31:** 589–599

Vert G, Grotz N, Dédaldéchamp F, Gaymard F, Guerinot ML, Briat JF, Curie C (2002) IRT1, an *Arabidopsis* transporter essential for iron uptake from the soil and for plant growth. Plant Cell **14:** 1223–1233

Wang N, Cui Y, Liu Y, Fan H, Du J, Huang Z, Yuan Y, Wu H, Ling HQ (2013) Requirement and functional redundancy of Ib subgroup bHLH proteins for iron deficiency responses and uptake in *Arabidopsis thaliana*. Mol Plant **6:** 503–513

Waters BM, Chu HH, Didonato RJ, Roberts LA, Eisley RB, Lahner B, Salt DE, Walker EL (2006) Mutations in Arabidopsis yellow stripe-like1 and yellow stripe-like3 reveal their roles in metal ion homeostasis and loading of metal ions in seeds. Plant Physiol **141:** 1446–1458

Williams LE, Pittman JK (2010) Dissecting pathways involved in manganese homeostasis and stress in higher plant cells. *In* R Hell, RR Mendel, eds, Cell Biology of Metals and Nutrients. Plant Cell Monographs, **Vol 17**. Springer-Verlag, Berlin, pp 95–117

Wu H, Chen C, Du J, Liu H, Cui Y, Zhang Y, He Y, Wang Y, Chu C, Feng Z, et al (2012) Co-overexpression FIT with AtbHLH38 or AtbHLH39 in Arabidopsis-enhanced cadmium tolerance via increased cadmium sequestration in roots and improved iron homeostasis of shoots. Plant Physiol **158:** 790–800

Yi Y, Guerinot ML (1996) Genetic evidence that induction of root Fe(III) chelate reductase activity is necessary for iron uptake under iron deficiency. Plant J **10:** 835–844

Yuan HM, Xu HH, Liu WC, Lu YT (2013) Copper regulates primary root elongation through PIN1-mediated auxin redistribution. Plant Cell Physiol **54:** 766–778

Yuan Y, Wu H, Wang N, Li J, Zhao W, Du J, Wang D, Ling HQ (2008) FIT interacts with AtbHLH38 and AtbHLH39 in regulating iron uptake gene expression for iron homeostasis in Arabidopsis. Cell Res **18:** 385–397

Yunta F, García-Marco S, Lucena JJ, Gómez-Gallego M, Alcázar R, Sierra MA (2003) Chelating agents related to ethylenediamine bis(2-hydroxyphenyl)acetic acid (EDDHA): synthesis, characterization, and equilibrium studies of the free ligands and their Mg^{2+}, Ca^{2+}, Cu^{2+}, and Fe^{3+} chelates. Inorg Chem **42:** 5412–5421

Zamioudis C, Hanson J, Pieterse CMJ (2014) β-Glucosidase BGLU42 is a MYB72-dependent key regulator of rhizobacteria-induced systemic resistance and modulates iron deficiency responses in Arabidopsis roots. New Phytol **204:** 368–379

Zhai Z, Gayomba SR, Jung HI, Vimalakumari NK, Piñeros M, Craft E, Rutzke MA, Danku J, Lahner B, Punshon T, et al (2014) OPT3 is a phloem-specific iron transporter that is essential for systemic iron signaling and redistribution of iron and cadmium in *Arabidopsis*. Plant Cell **26:** 2249–2264